

# Waveguide-integrated optical modulators with two-dimensional materials

Haitao Chen<sup>1,2,3</sup>, Hongyuan Cao<sup>1</sup>, Zejie Yu<sup>1</sup>, Weike Zhao<sup>1</sup>, and Daoxin Dai<sup>1,4,†</sup>

<sup>1</sup>State Key Laboratory for Modern Optical Instrumentation, College of Optical Science and Engineering, International Research Center for Advanced Photonics, Zhejiang University, Zijingang Campus, Hangzhou 310058, China

<sup>2</sup>College of Advanced Interdisciplinary Studies & Hunan Provincial Key Laboratory of Novel Nano-Optoelectronic Information Materials and Devices, National University of Defense Technology, Changsha 410073, China

<sup>3</sup>Nanhu Laser Laboratory, National University of Defense Technology, Changsha 410073, China

<sup>4</sup>Ningbo Research Institute, Zhejiang University, Ningbo 315100, China

**Abstract:** Waveguide-integrated optical modulators are indispensable for on-chip optical interconnects and optical computing. To cope with the ever-increasing amount of data being generated and consumed, ultrafast waveguide-integrated optical modulators with low energy consumption are highly demanded. In recent years, two-dimensional (2D) materials have attracted a lot of attention and have provided tremendous opportunities for the development of high-performance waveguide-integrated optical modulators because of their extraordinary optoelectronic properties and versatile compatibility. This paper reviews the state-of-the-art waveguide-integrated optical modulators with 2D materials, providing researchers with the developing trends in the field and allowing them to identify existing challenges and promising potential solutions. First, the concept and fundamental mechanisms of optical modulation with 2D materials are summarized. Second, a review of waveguide-integrated optical modulators employing electro-optic, all-optic, and thermo-optic effects is provided. Finally, the challenges and perspectives of waveguide-integrated modulators with 2D materials are discussed.

**Key words:** optical modulation; two-dimensional (2D) materials; on-chip; waveguide

**Citation:** H T Chen, H Y Cao, Z J Yu, W K Zhao, and D X Dai, Waveguide-integrated optical modulators with two-dimensional materials[J]. *J. Semicond.*, 2023, 44(11), 111301. <https://doi.org/10.1088/1674-4926/44/11/111301>

## 1. Introduction

In the era of big data, the number of digits generated and consumed has been growing enormously. As a result, fast and efficient data transfer and processing are becoming increasingly important. Meanwhile, the conventional approach with electronic interconnects faces challenges to fulfill the ever-increasing demand due to limited bandwidth and high energy consumption<sup>[1]</sup>. In contrast, optical interconnects have been recognized as a promising technology enabling high-capacity, high-speed, and energy-efficient data transfer and processing. In recent years, various photonic integrated circuits (PICs) have been demonstrated successfully for optical interconnects at different scales, and silicon photonics has been recognized as one of the most promising technologies for realizing high-performance and large-scale PICs because of its complementary-metal-oxide-semiconductor (CMOS) compatibility and high integration density<sup>[2–6]</sup>. In the past few decades, various active and passive photonic devices on silicon have been realized by using monolithic and heterogeneous integration technologies<sup>[7–14]</sup>. Among them, optical modulators are one of the most important functional devices<sup>[15]</sup> to determine the upper limit of the whole optical system. However, due to the intrinsic optoelectronic response limits of the silicon material, it is still very challeng-

ing to achieve high-performance optical modulators with ultra-high speed, ultralow power consumption, high modulation efficiency, and compact footprint on silicon chips<sup>[16–19]</sup>. One of the promising potential solutions is to utilize heterogeneous integration with the assistance of other excellent optoelectronic materials, such as metals<sup>[20]</sup>, germanium<sup>[21]</sup>, and III–V compound semiconductors<sup>[22]</sup>. Unfortunately, high-quality crystal growth on silicon is usually technologically challenging due to the mismatch of the lattice constants and the thermal expansion coefficients<sup>[23]</sup>.

Alternatively, two-dimensional (2D) materials have attracted a lot of attention since the discovery of graphene<sup>[24]</sup> because 2D materials show a lot of excellent optoelectronic properties that do not exist in their three-dimensional counterparts. In the past few years, 2D materials have been recognized as promising candidates to revolutionize modern technologies in optoelectronics<sup>[25–29]</sup>. For example, graphene, consisting of a single-layer hexagonal-lattice carbon atom, shows a semi-metal band structure. Its charge carriers can be described as massless Dirac fermions, while the conduction electrons have a linear dispersion at the lower energies, providing many opportunities to study novel physical phenomena<sup>[30]</sup>. Up to now, a wide range of excellent properties in optoelectronics have been found in graphene<sup>[31]</sup>, such as high carrier mobility, high thermal conductivity, broadband optical absorption, tunable bandgaps, large optical nonlinearity, excellent mechanical stability, and so on. It has even been dubbed a "miracle" material. Inspired by graphene, many other 2D materials have been discovered and studied, including transi-

Correspondence to: D X Dai, [dxdai@zju.edu.cn](mailto:dxdai@zju.edu.cn)

Received 18 APRIL 2023; Revised 5 JUNE 2023.

©2023 Chinese Institute of Electronics

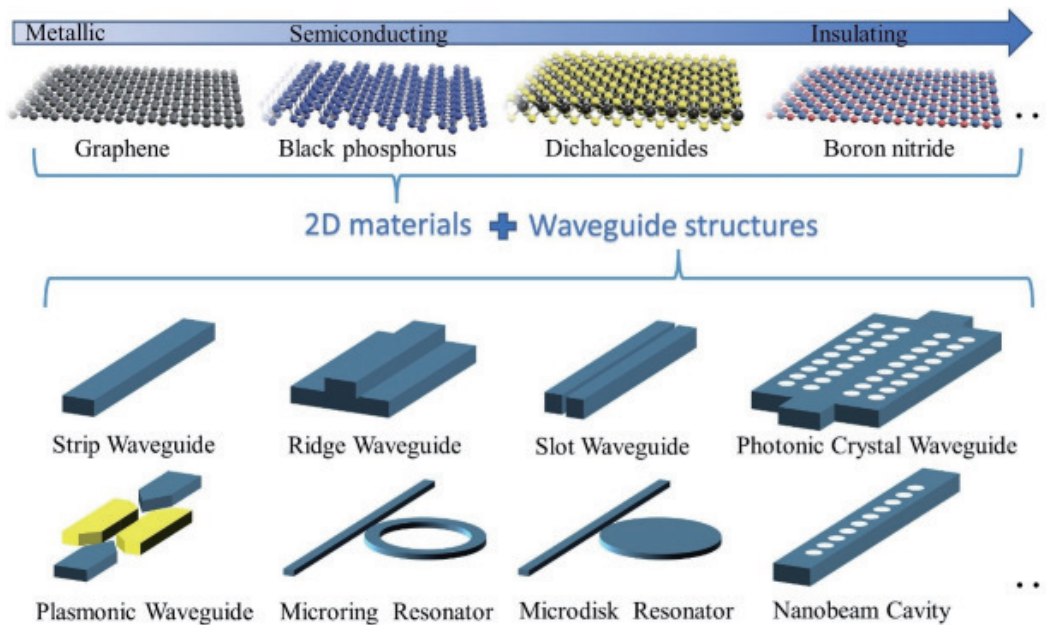


Fig. 1. (Color online) Schematic illustration of on-chip waveguide-integrated optical modulation combining various 2D materials and diverse waveguide structures; the upper part shows typical 2D materials ranging from semimetals to insulators, and the lower part shows typical waveguide structures.

tional metal dichalcogenides (TMDs)<sup>[27]</sup>, boron nitride<sup>[32]</sup>, black phosphorus (BP)<sup>[33]</sup>, and germanene<sup>[34]</sup>. They enrich the family of 2D materials and bring many opportunities for optoelectronics.

When using 2D materials for optical modulation, especially with on-chip optical waveguides, they show several attractive advantages. First, most 2D materials are mechanically robust with passivated surfaces, which can be readily integrated with waveguide structures without the lattice mismatch issues<sup>[35–37]</sup>. Second, the introduction of 2D materials has little influence on the modal field profiles of the optical waveguides because the layer is atomically thin<sup>[38–40]</sup>, which reduces the optical loss from unwanted mode mismatching and reflection. Third, instead of normal incident light on a 2D material sheet, in-plane propagation of light by integrating 2D materials on a waveguide usually allows a longer light-matter interaction length by utilizing the evanescent field of the guided optical mode, which will significantly improve the performance of 2D material optoelectronic devices. Fourth, the optical response of 2D materials covers a wide band of spectra, ranging from ultraviolet to terahertz (THz) or even to microwave frequency<sup>[31]</sup>, due to their diverse electronic band structures, which is highly desired for broadband optical modulation and some frequency spectra that are hard to realize effective modulation with conventional dielectric materials. Fifth, the optical response of 2D materials can be tuned in a wide range through electric gating<sup>[41, 42]</sup>, optical excitation<sup>[43, 44]</sup>, chemical doping<sup>[45]</sup>, or strain<sup>[46]</sup>, showing the potential to build high-quality optical modulation. Finally, heterostructures consisting of different kinds of 2D materials enrich the band structures of the 2D materials family. It is possible to obtain versatile functionalities that go beyond those of a single 2D material, as well as optical modulation with unprecedented high performance<sup>[47–51]</sup>. In addition, various waveguide structures, such as strip/ridge waveguides<sup>[52, 53]</sup>, slot waveguides<sup>[54, 55]</sup>, photonic crystal waveguides<sup>[56, 57]</sup>, plas-

monic waveguides<sup>[58, 59]</sup>, microring resonators (MRRs)<sup>[60, 61]</sup>, and nanobeam cavities<sup>[62, 63]</sup>, have been designed and implemented to enhance light-2D materials interactions. Thus, the combination of functional 2D materials and various waveguide structures could potentially realize high-performance on-chip optical modulation, as illustrated in Fig. 1. Indeed, on-chip waveguide-integrated optical modulators based on 2D materials have triggered lots of interest worldwide, and the field is still progressing rapidly.

In this article, we review the latest progress of on-chip waveguide-integrated optical modulators based on 2D materials, especially those that are compatible with the silicon photonics platform, including the strip/ridge waveguides, waveguide-coupled MRRs, photonic crystal waveguide, and plasmonic waveguides. The fundamental mechanisms of optical modulation with 2D materials are summarized at the beginning. Recent advances in waveguide-integrated optical modulators with 2D materials are then reviewed in terms of their operating principles, as well as the key figure of merit (FOM). Finally, the challenges of existing optical modulation with 2D materials and promising solutions are discussed. We have noted that several recent review articles on optical modulators based on 2D materials have been published<sup>[64–70]</sup>, whereas ours focuses on the waveguide-integrated form for integrated photonics and includes the most recent results, such as modulation utilizing bound states in the continuum (BIC) and plasmonic effects, which has not been done before and will provide complementary information for researchers.

## 2. Fundamentals of optical modulation

Generally, the optical response of materials can be described by the complex refractive index,  $\tilde{n} = n + ik$ , in which the real part represents the refractive index and the imaginary part reflects the absorption property. Optical modulation is usually realized by modulating the real or imaginary part of the complex refractive index of the materials in the

modulation region, which lays the foundation for optical modulation. Optical modulation can be categorized in many different ways. For example, various physical mechanisms have been utilized, and researchers have realized electro-optic modulators, all-optical modulators, thermo-optic modulators, magneto-optic modulators, acousto-optic modulators, mechano-optic modulators, and so on<sup>[17]</sup>. According to the attribute of light, researchers have developed intensity modulators, phase modulators, polarization modulators, and so on<sup>[66]</sup>. According to how the property of the materials change during light modulation, we can use refractive optical modulators and absorptive optical modulators. The typical physical effects for absorptive optical modulation include the saturable absorption<sup>[71]</sup>, the electro-absorption<sup>[72]</sup>, the Franz-Keldysh effect<sup>[17]</sup>, and so on, while the typical physical effects for refractive optical modulation include the Kerr effect<sup>[73]</sup>, the Pockels effect<sup>[17]</sup>, the thermal modulation<sup>[74]</sup>, and so on.

For optical modulators, the key FOMs include the modulation speed, the modulation depth (MD), the operation wavelength, the energy consumption, and the insertion loss (IL)<sup>[75]</sup>. The modulation speed is one of the most crucial parameters, determining how fast the data can be generated. In general, it is highly desirable to achieve optical modulators with a bandwidth up to tens of gigahertz (GHz) or even greater than 100 GHz for many high-speed applications, such as data transfer and microwave photonics. The MD is usually measured by the extinction ratio (the ratio between the maximum and minimum intensity of the modulated optical signal), which is usually characterized by the decibel (dB) unit. Given a modulation bandwidth, modulation with a higher MD helps lower the bit rate error of data transfer. In realistic applications, a certain level of MD (e.g., > 7 dB) is usually preferable for most areas. In some cases, such as passive mode-locking and short-distance transmissions, an MD of 4 dB is also feasible<sup>[17]</sup>. In addition, modulators with large MDs can be used to realize advanced modulation formats to further increase modulation speed. The operating wavelength of optical modulators is determined by their realistic applications. For optical data transfer systems, modulators are usually required to operate at one or more of the three major telecom windows (~0.86, 1.31, and 1.55  $\mu\text{m}$ ), and a broadband modulator is usually sought. With ever-increasingly large amounts of data to transmit and process, the energy consumption of optical modulation is becoming an increasingly critical issue, and many methods are being explored to reduce energy consumption per bit. It is expected that the energy consumption of efficient optical modulators will be two orders of magnitude lower compared to their electronic counterparts for on-chip interconnects<sup>[76]</sup>. IL, characterized as the loss of light after transmitting a modulator, is another important factor related to the system energy efficiency for realistic applications, and it usually comes from the material absorption and the scattering loss of optical waveguides. In addition, other characteristics of optical modulators, such as stability, footprint, fabrication cost, and compatibility, are also important considerations when evaluating overall performance for some applications.

For waveguide-integrated optical modulators with 2D materials, the light-2D material interaction is realized through the evanescent coupling between the 2D materials and silicon waveguides, where the complex refractive index of 2D

materials can be modulated by external excitations, such as electric gating and optical stimulus. Various types of waveguide-integrated optical modulators with 2D materials have been successfully demonstrated and have excellent performance. In the following sections, waveguide-integrated optical modulators based on 2D materials are reviewed concerning the key FOMs. In particular, we discuss modulation speed, MD, and energy consumption.

### 3. Waveguide-integrated optical modulation with 2D materials

For waveguide-integrated optical modulators, the device performance depends strongly on the choice of 2D materials, as well as waveguide structures. So far, graphene has been the most popular 2D material for waveguide-integrated optical modulators<sup>[17, 66]</sup>. Meanwhile, it is being extended to some other 2D materials, such as TMDs<sup>[77]</sup> and BP<sup>[78]</sup>. Meanwhile, various waveguide structures have been designed and implemented using a variety of common photonic platforms, including silicon, silicon nitride<sup>[77]</sup>, as well as chalcogenide glass<sup>[79]</sup>. Among them, silicon photonic waveguides are the most commonly used since silicon photonics have been recognized as the most promising mainstream technology for PICs and have been developed very successfully. In this section, a review of the state-of-the-art waveguide-integrated optical modulators with 2D materials is given, categorized by the driving mechanisms, including electro-optic, all-optic, and thermo-optic mechanisms. Particularly, we also review the recent progress of optical modulators with 2D materials hybridized with BIC structures.

#### 3.1. Electro-optic modulators with 2D materials

As one of the most widely-used devices in data communications, electro-optic modulators are usually realized by introducing a kind of material whose complex refractive index can be tuned by the change of carrier concentration and energy band. For 2D materials, the band structure is sensitive to the external electric field since the electrons are strongly confined in the out-of-plane direction due to their atomic thickness<sup>[80]</sup>. As a result, the electronic and optical properties can be tuned effectively by introducing an external electric field. For example, the optical transmission of graphene<sup>[81]</sup> and TMDs<sup>[82]</sup> can be substantially modified through electric gating. For waveguide-integrated electro-optic modulators with 2D materials, various structures have been implemented to achieve high-performance electro-optic modulators so far, including straight waveguides<sup>[16, 53, 83]</sup>, MZIs<sup>[84, 85]</sup> and MRRs<sup>[60]</sup>. Here we review the latest advances in on-chip waveguide-integrated electro-optic modulators, and their respective advantages and disadvantages.

##### 3.1.1. Electro-optic modulators based on strip/ridge waveguides

In 2011, Liu *et al.* demonstrated a broadband waveguide-integrated electro-optic modulator based on the electro-absorption effect of graphene for the first time. The structure of the device is schematically shown in the left-hand part of Fig. 2(a)<sup>[16]</sup>. A single layer of graphene was mechanically transferred onto a silicon-on-insulator waveguide. There was a thin  $\text{Al}_2\text{O}_3$  insulating layer between the graphene sheet and the silicon core, so that the Fermi level of graphene could be modulated when an electric field was applied through the



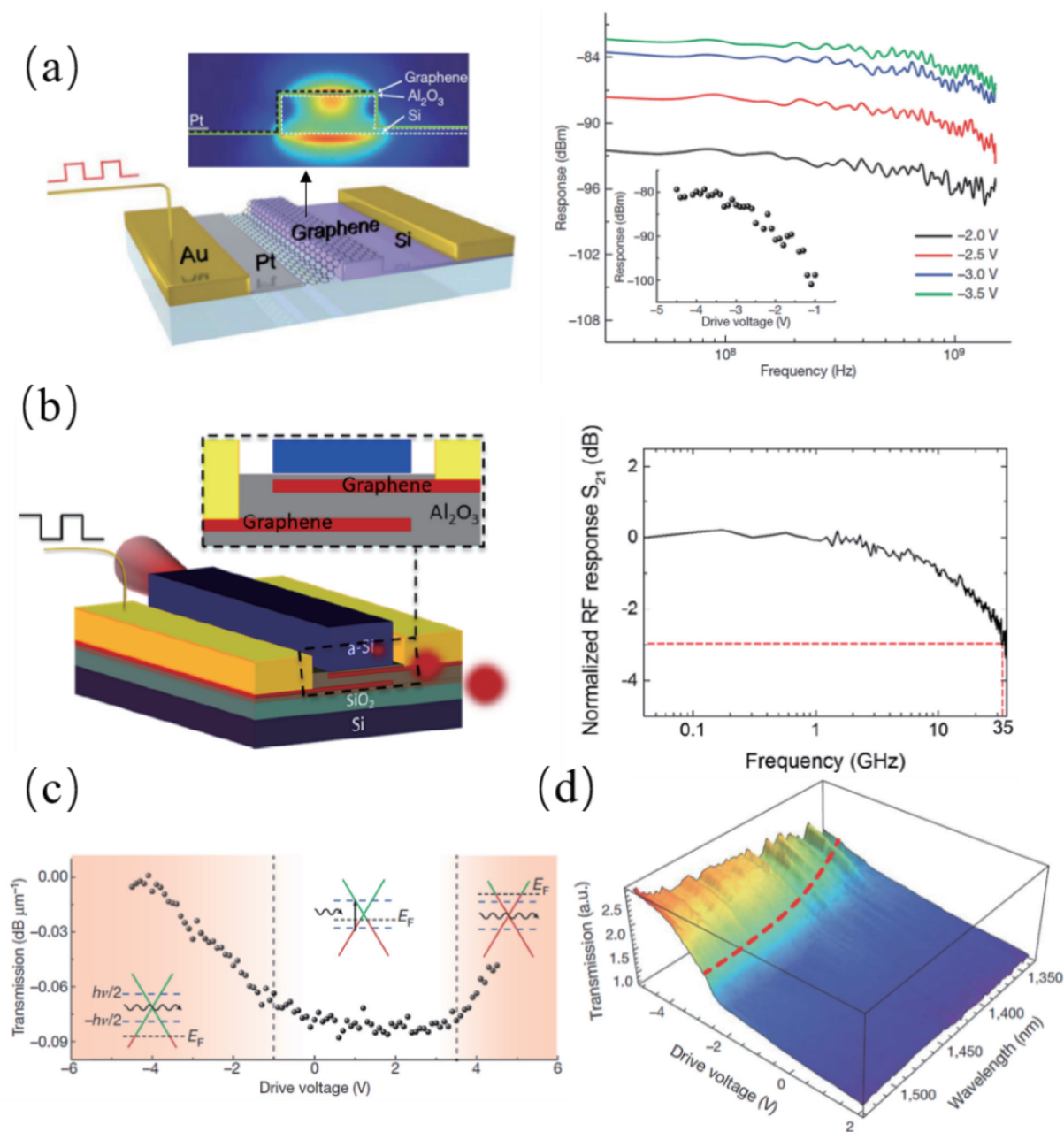


Fig. 2. (Color online) Waveguide-integrated electro-optic modulators with non-resonant structures. (a) Schematic illustration of the first waveguide-integrated broadband electro-optic modulators based on graphene (left-hand) and the dynamic response of the device under different bias voltages (right-hand). The waveguide was optimized to carry a single mode and achieve a strong light–matter interaction in graphene<sup>[16]</sup>. (b) Schematic configuration of a waveguide-integrated electro-optic modulator based on two layers of graphene separated by a dielectric spacer (left-hand) and the measured RF response (right-hand)<sup>[52]</sup>. (c) The voltage-dependent static electro-optic response of a single graphene layer<sup>[16]</sup>. (d) The transmission spectra of the device shown in part (a) as a function of the driving voltage<sup>[16]</sup>. Figures reproduced with permission: (a, c, d) Ref. [16], © 2011 Nature Publishing Group, (b) Ref. [52], © 2016 American Chemical Society.

gate electrodes. The waveguide was designed to improve the light absorption of graphene due to its enhanced evanescent field. This device provided a noticeable modulation efficiency of around 0.1 dB/μm in the communication band, while the bandwidth was limited to around 1 GHz due to the parasitic response of the driving circuit, as shown in the right-hand part of Fig. 2(a). To improve the performance of the on-chip electro-optic modulators, such as bandwidth, Dalir *et al.* have experimentally demonstrated a waveguide-integrated electro-optic modulator using a double-layer (DL) graphene structure and achieved a 3 dB bandwidth up to 35 GHz. The schematic structure and the radio frequency (RF)

response of the device are shown in Fig. 2(b)<sup>[52]</sup>. In this structure, the lower graphene layer acts as a tunable absorber, while the upper one functions as a transparent electrode gate. In addition, the DL structure can also greatly reduce the IL and increase the MD. Furthermore, Mohsin *et al.* have demonstrated an MD of 16 dB and an IL of 3.3 dB for a waveguide-integrated electro-optic modulator based on DL graphene<sup>[53]</sup> by carefully designing the geometry of the waveguide and optimizing the materials transfer process. To further enhance the modulation speed and efficiency simultaneously, Hitesh *et al.* demonstrated 2D–3D dielectric integration in a high-quality encapsulated graphene-based electro-



optic modulator<sup>[86]</sup>, where hafnium oxide (HfO<sub>2</sub>) and two-dimensional hexagonal boron nitride (hBN) were applied in the insulating section of a DL graphene electro-absorption modulator. They achieved a modulation bandwidth of ~39 GHz and highly improved modulation efficiency. According to the theoretical prediction, a 3 dB bandwidth of 120 GHz could be achieved in DL structures<sup>[87]</sup>, which indicates that there is still a lot of room for further optimization. The underlying mechanism for these electro-optic modulators is gate-dependent absorption, as illustrated in Fig. 2(c)<sup>[16]</sup>. As is well known, graphene is quite absorptive through the interband transition when the Fermi level of graphene is less than half of the incident photon energy (middle regime of Fig. 2(c)). When the Fermi level is tuned to be lower (left-hand regime of Fig. 2(c)) or higher (right-hand regime of Fig. 2(c)) than the half-photon energy, either there are no electrons available for an interband transition or all electron states in resonance with incident photons are fully occupied, and thus the interband transition is forbidden, leading to the reduction of the absorption. In principle, because of the semi-metal band structure of graphene and the large modulation range of its Fermi level, graphene modulators can work in a broadband wavelength spectrum, from visible light to THz waves. The device shown in Fig. 2(a) demonstrated a 3-dB modulation in the spectral range from 1350 to 1600 nm, as shown in Fig. 2(d), and the operation wavelength range for the modulation is expected to be broadened by improving the driving voltages.

Many other efforts have been made to improve the performance of waveguide-integrated graphene electro-optic modulators by using different waveguide configurations, including graphene-on-silicon slot waveguides<sup>[54, 55]</sup>, graphene-embedded waveguides<sup>[88, 89]</sup>, and mode engineering<sup>[90]</sup>. Therefore, it can be expected that FOMs of waveguide-integrated electro-optic modulators with 2D materials will be continually improved toward realistic applications after exploring new structures and materials.

### 3.1.2. Electro-optic modulators based on resonant structure

Although waveguide-integrated optical modulators based on electro-optic absorption show good performance in some aspects of modulation, the light-matter interaction strength is still relatively weak due to the atomic thickness of 2D materials, which limits the performance of such absorption-based modulators. Therefore, waveguide-integrated resonant and interferometric structures have been implemented to improve the key characteristics. Here, we review the latest progress in waveguide-integrated electro-optic modulators based on 2D materials with resonant and interferometric structures.

In 2014, Qiu *et al.* demonstrated an electro-optic modulator by covering single-layer graphene on top of a silicon MRR, demonstrating an MD of around 40% at 1.55  $\mu\text{m}$ <sup>[91]</sup>. The IL was high because the graphene covered the entire surface of the resonator. To reduce the IL, a silicon MRR partially covered by graphene was later demonstrated, allowing an MD of up to 12.5 dB<sup>[92]</sup>. In 2015, Phare *et al.* demonstrated an electro-optic modulator based on an MRR structure working under critical coupling condition<sup>[60]</sup>, as shown in Fig. 3(a). When the voltage was applied, the absorption in graphene

decreased, and the cavity resonance changed from under coupling to near-critical coupling (right part in Fig. 3(a)). Thus, the transmission through the bus waveguide was modulated significantly. By carefully designing the structure, the device shows a 3-dB bandwidth as wide as 30 GHz and an MD of 15 dB. The modulation efficiency for this device was as high as 1.5 dB/V, and the energy consumption was around 800 fJ/bit. Moreover, the theoretical investigation has shown that the performance of such optical modulators can be further improved by optimizing the design<sup>[93]</sup> and that the spectral response can be extended to the THz regime<sup>[94]</sup>.

An interferometric structure is another platform that is widely used to build electro-optic modulators. Various interferometric architectures have been designed<sup>[95–97]</sup> to realize high-performance graphene-based optical modulation. In 2015, Mohsin *et al.* experimentally demonstrated an electro-optic phase modulator by integrating a gated graphene layer in the silicon waveguide of an MZI<sup>[98]</sup>. The key parameters of the phase modulators were well characterized by extracting information from interference patterns. In 2018, Soriano *et al.* reported a graphene-silicon phase modulator with gigahertz bandwidth. A picture of the fabricated device is shown in Fig. 3(b)<sup>[85]</sup>. By gating the graphene under a proper voltage, the real part instead of the imaginary part dominates the variation of the refractive index of graphene, thus resulting in effective phase modulation. For this device, the MD is as large as 35 dB and the modulation efficiency is about 0.28 V-cm under static driving, which outperformed the state-of-the-art silicon optical modulators relying on p-n junctions and can be used in both analog and digital circuits<sup>[85]</sup>. Recently, Cheng *et al.* demonstrated a photonic crystal waveguide-integrated electro-optic modulator based on DL graphene<sup>[56]</sup>. By covering DL graphene onto slow-light silicon photonic crystal waveguides, this device has a bandwidth of 12 GHz, while the MD was only 0.55 dB for a 10- $\mu\text{m}$ -long device, which was far less than the simulated value of 0.5 dB/ $\mu\text{m}$ . Therefore, more efforts are still required to optimize the fabrication processes of photonic crystal waveguide-based graphene electro-optic modulators<sup>[56]</sup>.

Importantly, the 2D materials used to construct waveguide-integrated electro-optic modulators have extended from graphene to other 2D materials, which show extraordinary performance in some aspects of electro-optic modulation. Recently, Datta *et al.* demonstrated an electro-optic modulator based on a TMDs-integrated MZI structure<sup>[77]</sup>, as shown in Fig. 3(c). Here, the monolayer WS<sub>2</sub>-SiN waveguide has an ionic liquid cladding. When gated properly, the monolayer WS<sub>2</sub> was heavily doped by the ionic liquid, resulting in a dramatic change in the real part of the refractive index but little change in the imaginary part. An electrostatically gated SiN-WS<sub>2</sub> phase modulator with a high modulation efficiency of 0.8 V-cm was demonstrated based on an MZI structure, which outperforms the state-of-the-art lithium niobate modulators. The normalized transmission spectra of the modulator with different voltages applied to the long arm of the MZI are shown in the right-hand part of Fig. 3(c). The demonstrated waveguide-integrated electro-optic modulator using TMDs opens new avenues beyond graphene, inspiring new explorations of 2D materials-based electro-optic modulators.

Overall, on-chip waveguide-integrated electro-optic modulators with 2D materials have shown extraordinary proper-

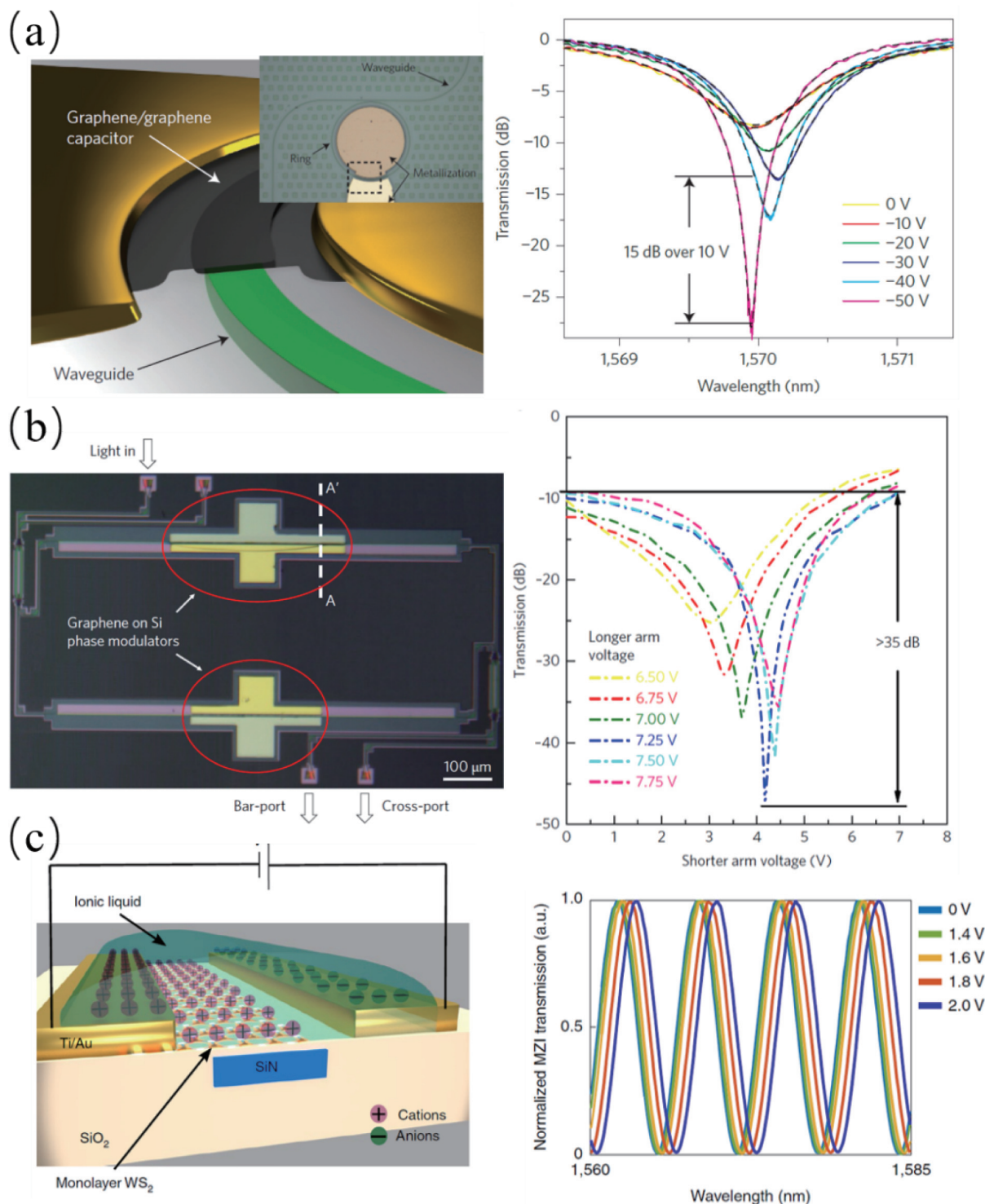


Fig. 3. (Color online) Waveguide-integrated electro-optic modulators with resonant and interferometric structures. (a) Schematic illustration of an electro-optic modulator based on graphene-integrated MRR (left-hand) and its transmission spectra at different gate voltages (right)<sup>[60]</sup>. The upper-right-hand inset of the left-hand picture shows the microscope image of the fabricated structure. (b) Optical microscope image of a graphene-based modulator with an MZI structure (left-hand) and its transmission spectra at different gate voltages (right-hand)<sup>[85]</sup>. (c) Schematic illustration of a composite SiN-WS<sub>2</sub> waveguide with ionic liquid ([P14+][FAP-]) cladding used as an active region for electro-optic modulators based on an MZI structure (left-hand), and the transmission spectra of the device at different gate voltages (right-hand)<sup>[77]</sup>. Figures reproduced with permission: (a) Ref. [60], © 2015 Nature Publishing Group. (b) Ref. [85], © 2018 Nature Publishing Group. (c) Ref. [77], © 2020 Nature Publishing Group.

ties and are promising for realistic applications. A summary of the performances of the major reported devices is given in Table 1. However, there remain challenges. At first, 2D materials have high carrier mobility and could potentially enable extremely fast optical modulation. For example,

graphene has been predicted to be able to realize modulation bandwidth beyond 100 GHz<sup>[87, 105]</sup>. However, the experimentally demonstrated value so far is only a few tens of GHz (~40 GHz<sup>[86, 104]</sup>), which is limited by the parasitic response that depends on the configuration of the devices. Therefore,

Table 1. Performance of typical on-chip waveguide-integrated electro-optic modulators.

Materials <sup>a)</sup>	Structure <sup>b)</sup>	Bandwidth <sup>c)</sup> (GHz)	Modulation depth (dB)	Insertion loss (dB)	Energy consumption (fJ/bit)	Drive voltage (V)	Ref. <sup>d)</sup>	Time
SL Gr	Si waveguide	1.2	4	—	—	~3.5	[16]	2011
BL Gr	Si waveguide	1	6.5	4	—	~5	[83]	2012
BL Gr	Si waveguide	120*	2.9*	2.5*	—	8	[87]*	2012
ML Gr	Si waveguide	100*	34*	—	17.6*	—	[99]*	2014
BL Gr	Si waveguide	1.8	16	3.3	—	6	[53]	2014
SL Gr	Si MRR	80*	2.2*	—	—	6	[91]*	2014
BL Gr	Si <sub>3</sub> N <sub>4</sub> MRR	30	22	8.5	800	10	[60]	2015
SL Gr	SiMRR	—	6.8	18	—	4	[92]	2015
Gr/hBN	Si PhC cavity	1.2	3.2	—	—	2.5	[100]	2015
BL Gr	a-Si waveguide	35	2	0.9	1400	25	[52]	2016
SL Gr	Si waveguide	6	5	3.8	350	2.5	[101]	2016
BL Gr	Si waveguide	120*	$\pi^*$	—	452*	6*	[102]*	2017
BL Gr	Plasmonic waveguide	—	0.13 dB/ $\mu$ m	—	—	7.5	[58]	2017
SL Gr	Si MZI	5	35	—	1000	2	[85]	2018
BL Gr	Dielectric waveguide	5	3	—	—	6	[103]	2019
SL WS <sub>2</sub>	Si <sub>3</sub> N <sub>4</sub> MZI	0.3	3	—	—	8	[77]	2020
BL Gr	Si waveguide	39	4.4	7.8	160	3.5	[86]	2021
BL Gr	Si slot MRR	>40	33	5.8	—	6	[104]	2022

<sup>a)</sup> Gr, Graphene; SL, single layer; BL, bilayer; ML, multilayer; hBN, hexagonal boron nitride. <sup>b)</sup> MRR, microring resonator; PhC, photonic crystal; a-Si, amorphous silicon; MZI, Mach-Zehnder interferometer. <sup>c)</sup> Bandwidth indicates a 3 dB cutoff frequency. <sup>d)</sup> Values and references marked with \* refer to the calculated results.

there is plenty of room to improve the modulation bandwidth, and great efforts in both the design and fabrication of devices are required. In terms of the MD, one should realize that it highly depends on the modulation configurations. For the direct amplitude modulation, the absorption change originates from the gate-tuned interband transitions. The currently demonstrated devices showed an MD from a few dB<sup>[16, 52, 83]</sup> to more than 10 dB<sup>[53, 60]</sup>. For resonator- or MZI-based modulators, the MD depends on both the extinction ratio and the phase shift induced by the external excitation. When using a cavity with critical coupling or an MZI with a well-balanced between the two arms, the MD can be enormous<sup>[61, 106]</sup>. As for the IL, the source mainly comes from the absorption or scattering of 2D materials and the excessive loss of the waveguiding structures. In an ideal case, the IL caused by graphene can be reduced to an extremely small value by utilizing electrically gated structures<sup>[107]</sup>. For waveguide-integrated electro-optic modulators<sup>[52]</sup>, an IL of less than 1 dB has been achieved. Energy consumption per bit is becoming increasingly important for optical interconnects, particularly for ultrahigh-speed optical communication in the future, which is primarily determined by the drive voltage and the capacitance as  $E = CV^2/4$ . Since the drive voltage  $V$  is inversely proportional to the capacitance  $C$ , the energy consumption is proportional to  $V$  or  $1/C$ <sup>[66]</sup>. As a result, one has to increase the capacitance or decrease the drive voltage to achieve lower energy consumption, which depends on the material properties and the structural design. For example, in the structure consisting of dual-layered graphene<sup>[87]</sup>, the capacitance is proportional to the dielectric constant of the oxide dielectric layer and inverse to the distance, in which an oxide layer with large dielectric constant should be chosen and the thickness should be as thin as possible to lower the energy

consumption. However, it should be noted that increasing the capacitance  $C$  will decrease the modulation bandwidth, thus these two interplayed parameters need to be well balanced when designing the modulators. The reported energy consumption for waveguide-integrated electro-optic modulators ranges from tens to hundreds of fJ/bit, either theoretically<sup>[99, 102]</sup> or experimentally<sup>[60, 101]</sup>, while the predicted energy consumption can be down to a few fJ/bit<sup>[76]</sup>. For the operation wavelength range, a non-resonant structure usually supports a wideband working spectrum, while the working wavelength range for resonant structures is usually quite narrow. It should be noted that the FOMs of optical modulators are highly interplayed parameters. For example, a stronger light-matter interaction is usually required to improve the MD, which might result in a higher IL. Therefore, a trade-off is generally required when designing optical modulators for realistic applications<sup>[66]</sup>.

### 3.2. All-optical modulators with 2D materials

For all-optical modulation, the signal light is modulated by another light beam, which possibly offers ultrafast and broadband optical signal processing and has attracted a lot of attention<sup>[64, 67, 108]</sup>. In particular, there are strong nonlinear optical effects in some 2D materials, and thus all-optical modulation based on 2D materials has exhibited extraordinary properties, including saturable absorbers<sup>[109–111]</sup>, wavelength converters<sup>[112]</sup>, optical limiters<sup>[113]</sup>, and polarization controllers<sup>[114]</sup>. Due to the demand for on-chip ultrafast all-optical signal processing, waveguide-integrated all-optical modulation has increasingly attracted attention<sup>[64]</sup> and great progress has been achieved.

In 2014, Yu *et al.* reported an all-optical modulator in a hybrid graphene-silicon waveguide structure based on opti-



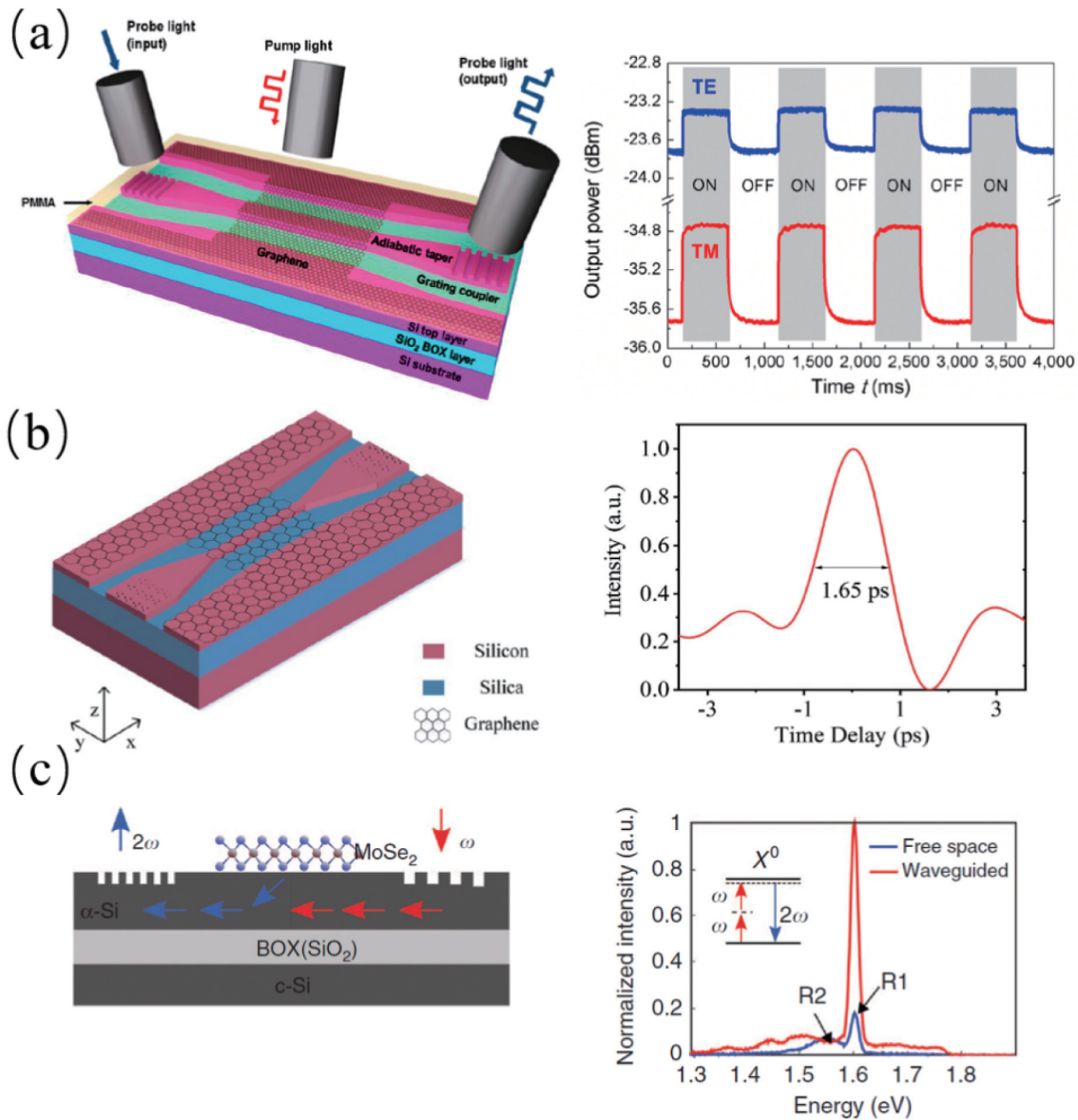


Fig. 4. (Color online) Waveguide-integrated all-optical modulators with 2D materials. (a) Schematic illustration of a waveguide-integrated all-optical modulator with graphene based on the OIT effect (left-hand) and its dynamic response for different polarizations with a local modulated optical pump (right-hand)<sup>[115]</sup>. (b) Schematic structure of a waveguide-integrated all-optical modulator with graphene based on the saturable absorption effect (left-hand) and the transmission spectra of the probe light as a function of its time delay relative to the pump light (right-hand)<sup>[118]</sup>. (c) Schematic illustration of a waveguide-integrated all-optical wavelength converter based on monolayer MoSe<sub>2</sub> (left-hand) and the measured second-harmonic generation signal from the waveguide-integrated structure compared to the free space excitation case (right-hand)<sup>[119]</sup>. Figures reproduced with permission: (a) Ref. [115], © 2014 American Chemical Society. (b) Ref. [118], © 2020 Chinese Laser Press. (c) Ref. [119], © 2017 Nature Publishing Group.

cally induced transparency (OIT) effects<sup>[115]</sup>, which can operate over a broad wavelength range. The schematic structure of the device is shown in Fig. 4(a), where monolayer graphene was transferred onto a predefined silicon ridge waveguide. It was verified that the OIT effect occurred when the pump light was on, and thus the transmission of the signal light can be effectively modulated by an external pump light. Interestingly, the modulation can even be achieved when the illuminated light is far away from the waveguide region. Further study showed that a Schottky diode was formed when a graphene sheet was put on top of the silicon layer, and the carrier transport between the graphene and the silicon layer was the underlying mechanism for the observed OIT effect. Later, based on the OIT effect, all-optical

modulation with graphene on a silicon photonic crystal cavity was demonstrated<sup>[57]</sup>. By introducing a control laser focusing on the photonic cavity, a 3.5-nm resonance-wavelength shift and 20% change in the quality factor were realized at 1.55  $\mu\text{m}$ <sup>[57]</sup>. Inspired by the ultrafast fiber laser based on the saturable absorption effects of graphene, the nonlinear response of graphene integrated onto waveguide structures has been studied theoretically<sup>[63, 116]</sup> and experimentally<sup>[117]</sup>. Wang *et al.* demonstrated an all-optical modulator with a hybrid graphene-silicon waveguide based on the saturable absorption effect<sup>[118]</sup>, as shown in Fig. 4(b). The reported MD is 22.7% with a saturation threshold of 1.38 pJ per pulse and the measured response time is around 1.66 ps, which shows the potential for applications in ultrafast on-chip all-optical

Table 2. Performance of typical on-chip waveguide-integrated all-optical modulators.

Materials <sup>a)</sup>	Structures <sup>b)</sup>	Principle <sup>c)</sup>	Response time (ps)	Modulation depth (dB)	energy consumption <sup>d)</sup>	Ref. <sup>e)</sup>	Publication time
SL Gr	Si waveguide	OIT	–	1	2 W/cm <sup>2</sup>	[115]	2014
SL Gr	Si PhC cavity	OIT, hot carrier effects	–	–	10 kW/cm <sup>2</sup>	[57]	2015
SL WS <sub>2</sub>	Si <sub>3</sub> N <sub>4</sub> waveguide	PL	–	>10	–	[120]	2017
SL Gr	Dielectric waveguide	OIT	–	2.75	–	[1]	2018
SL WSe <sub>2</sub>	Plasmonic waveguide	third-order nonlinearity	0.29	~0.3	650 fJ/bit	[121]	2019
SL Gr	Plasmonic waveguide	–	–	2.1	–	[122]	2019
SL Gr	Si waveguide	SA	1.65	1.1	2100 fJ/bit	[118]	2020
SL Gr	Plasmonic waveguide	SA	0.26	3.5	35 fJ/bit	[59]	2020
SL Gr	Plasmonic waveguide	SA	0.03–0.12*	3.5*	<600* fJ/bit	[123]*	2021
Gr/hBN	Si slot waveguide	SA	0.6*	7.3*	<326* fJ/bit	[124]*	2022

<sup>a)</sup> Gr, Graphene; SL, single layer; hBN, hexagonal boron nitride. <sup>b)</sup> PhC, photonic crystal. <sup>c)</sup> OIT, optically induced transparency; PL, photoluminescence; SA, saturable absorption. <sup>d)</sup> The unit W/cm<sup>2</sup> refers to the power density of the pumped light. <sup>e)</sup> Values and references marked with \* refer to the calculated results.

modulation with low energy consumption. In addition, 2D materials-based all-optical modulation has been extended from graphene to other 2D materials. For example, the TMDs-waveguide has also been demonstrated to effectively enhance the second harmonic generation from monolayer MoSe<sub>2</sub>, as shown in Fig. 4(c)<sup>[119]</sup>. This shows that the second-order nonlinear response of the silicon waveguide could be dramatically enhanced through integration with 2D TMDs, which is of great significance for silicon photonics since second-order nonlinearity is absent in silicon itself. Yang *et al.* have demonstrated an all-optical modulator by integrating monolayer WS<sub>2</sub> onto a Si<sub>3</sub>N<sub>4</sub> optical waveguide, in which a 640 nm signal light was effectively modulated and amplified by a 532 nm modulated light based on the photoluminescence from WS<sub>2</sub><sup>[120]</sup>.

Generally, great efforts have been made toward ultrafast and energy-efficient all-optical modulators, and a brief list of the performance of the representative studies is shown in Table 2. For all-optical modulators, the response time is usually determined by the intrinsic response of 2D materials. As a result, the modulation response can be as fast as a few picoseconds<sup>[125, 126]</sup> or even sub-picoseconds<sup>[59, 127]</sup>, indicating an ultrafast modulation speed up to hundreds of GHz or even THz. Currently, all-optical modulators have been reported with response times ranging from a few picoseconds<sup>[118, 126]</sup> to a few hundred femtoseconds<sup>[59]</sup>. Thus, all-optical modulation is one of the fastest (if not the only) modulation schemes. In terms of MD, the demonstrated devices<sup>[118]</sup> show only a few dB, which needs to be improved further for realistic applications. Due to the relatively high threshold, nonlinear effect-based all-optical modulators usually have a higher energy consumption compared to electric ones. Thus, novel structures or mechanisms are required to lower energy consumption<sup>[66]</sup>. For example, novel materials with high nonlinear coefficient and plasmonic structures with a highly enhanced local field can be adopted to decrease the energy consumption of all-optical modulators.

### 3.3. Thermo-optic modulators with 2D materials

Thermo-optic modulation relies on the temperature dependence of the refractive index of waveguide materials and has been widely used in silicon PICs<sup>[128, 129]</sup>. Metal

heaters are usually used for thermally tuning photonic devices. In this case, a relatively thick low-index upper-cladding layer is usually needed to isolate the metal absorption, which, however, induces several drawbacks. The low-index upper-cladding usually has poor heat conductivity, resulting in slow response and low heating efficiency. One might notice that the core region is much colder than the metal heater, and thus the temperature dynamics for the core region are quite limited due to the limitation for the temperature of the metal heater itself.

Alternatively, graphene has been recognized to be an attractive choice for transparent nano-heaters because of its high thermal conductivity (up to 5300 W/(m·K)) at room temperature<sup>[130]</sup> and high optical damage threshold. More importantly, graphene is ultra-thin enough to be almost transparent and introduces very little influence on the guided modes in an optical waveguide<sup>[61, 131, 132]</sup>.

In 2014, a transparent graphene nano-heater for silicon photonic waveguides was proposed and demonstrated for the first time<sup>[133]</sup>, in which case the graphene nano-heater touches with the silicon core directly, enabling fast and efficient thermal conduction. As demonstrated, the graphene nano-heater has a higher heating efficiency, faster response speed, and a larger thermal dynamic range than traditional metal micro-heaters. A thermally-tunable microdisk resonator was demonstrated with such a transparent graphene nano-heater<sup>[134]</sup>. Fig. 5(a) shows the thermally-tunable silicon microdisk resonator with transparent graphene nano-heaters and the measured spectral responses<sup>[134]</sup>. It can be seen that the resonant wavelength  $\lambda_{\text{res}}$  has a red-shift of  $\Delta\lambda = \sim 5$  nm when the heating power  $P_{\text{heating}}$  is 10.5 mW. In Ref. [61], a silicon microring resonator was demonstrated with a wide graphene heater covering the whole structure, as shown in Fig. 5(b). The measurement results for the resonant wavelength and the quality factor are also shown as a function of the applied voltage. In this case, the resonant wavelength of the MRR shifts by 2.9 nm with a large MD of 7 dB when the heating power is 28 mW (the bias voltage is 7 V). Later on, the transparent graphene nano-heater on silicon was also used successfully to realize a thermo-optic Mach–Zehnder optical switches with slow-light nanostructures<sup>[135]</sup>. In conclusion, this transparent graphene nanoheater provides a promising

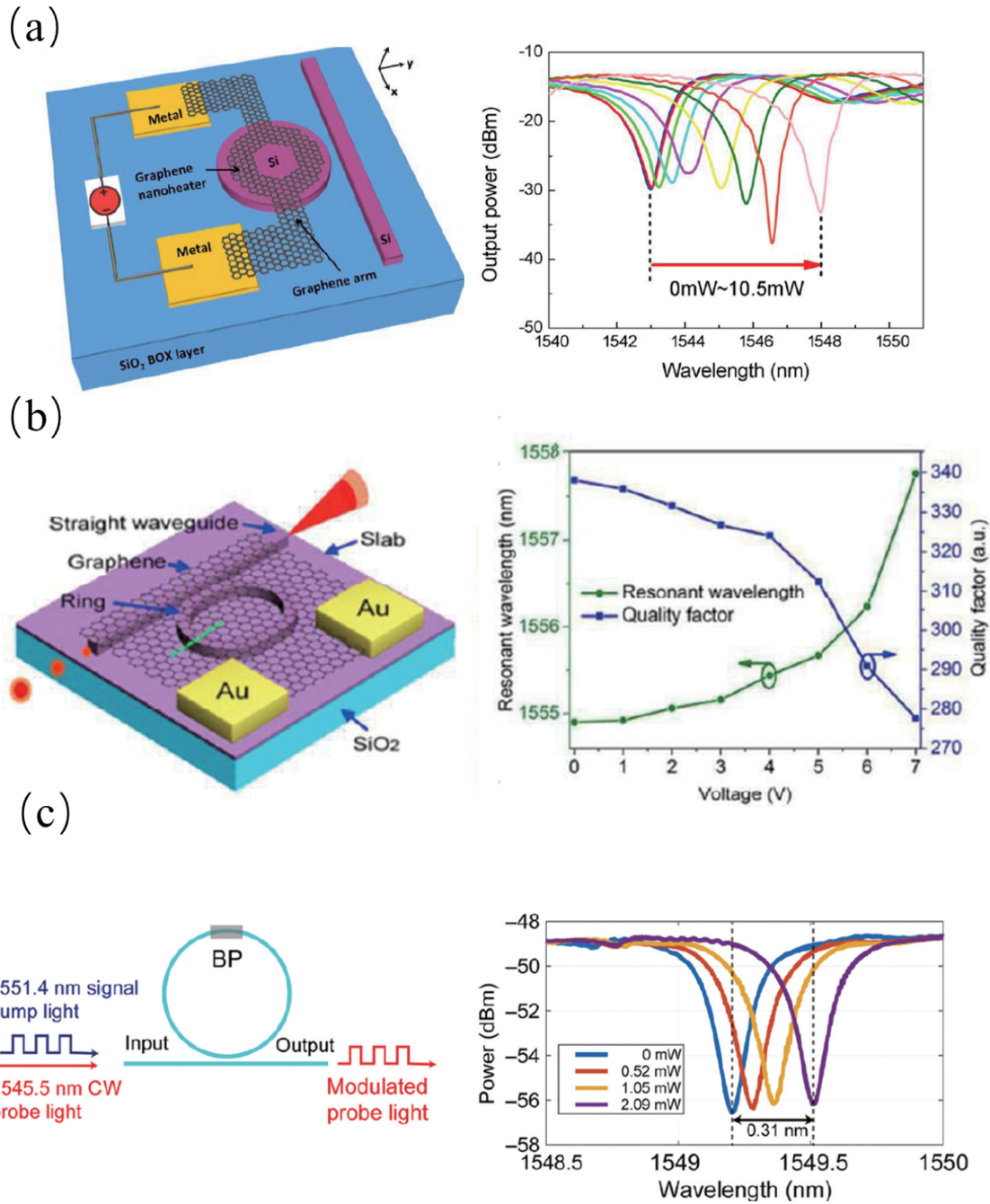


Fig. 5. (Color online) Waveguide-integrated thermo-optic modulators based on 2D materials. (a) Schematic illustration of an optical modulator with a resonator using a graphene nano-heater (left-hand) and the output spectra of the device operating with different heating powers (right-hand)<sup>[139]</sup>. (b) Schematic illustration of a thermo-optic modulator with an MRR structure using a graphene heater (left-hand), and the measured resonant wavelength and the Q factor when operating at different applied voltages<sup>[61]</sup>. (c) Schematic illustration of a thermo-optic modulator with an MRR using the photothermal effect in BP (left-hand) and the measured resonant wavelength for different pumping powers (right-hand)<sup>[78]</sup>. Figures reproduced with permission: (a) Ref. [139], © 2014 AIP Publishing. (b) Ref. [61], © 2015 Royal Society of Chemistry. (c) Ref. [78], © 2020 De Gruyter.

option to realize efficient thermally-tunable silicon photonic devices. It is possible to further improve the heating efficiency  $\eta_d (= \Delta\lambda/P_{\text{heating}})$  by reducing the heating volume.

In addition to the electrically induced thermal effect, the photothermal effect, where the temperature change is induced by light pumping, has also been applied to realize thermo-optic modulation<sup>[78, 136, 137]</sup>. For example, Cheng *et al.* recently demonstrated a thermo-optic modulator using the photothermal effect of BP<sup>[78]</sup>, with a response time of less than 1  $\mu$ s. A schematic of the device and the spectral

response under different pumping powers are shown in Fig. 5(c). These results show that 2D materials are promising to be used as micro-heaters or micro-conductors for optical modulators. Recently, Cao *et al.* demonstrated an efficient and fast all-optical modulator based on *in-situ* grown MoTe<sub>2</sub> nanosheets on silicon structures, utilizing the thermo-optic effect of MoTe<sub>2</sub>, paving the way for large-scale integration of 2D materials onto a silicon photonic platform<sup>[138]</sup>. In addition, the chalcogenide-glass waveguide provides another versatile platform to integrate 2D materials for various applications. A



Table 3. Performance of typical on-chip waveguide-integrated thermo-optic modulators.

Materials <sup>a)</sup>	Scheme	Structures <sup>b)</sup>	Rise/fall time ( $\mu\text{s}$ ) <sup>c)</sup>	Tuning efficiency (nm/mW)	Ref.	Time
SL Gr	Electrothermal effect	Si MZI	20/20	0.0636	[139]	2014
SL Gr	Electrothermal effect	Si MRR	0.75/0.8	0.104	[61]	2015
SL Gr	Electrothermal effect	Si MDR	12.8/8.8	1.67	[134]	2016
SL Gr	Electrothermal effect	ChG PhC cavity	14/–	10	[79]	2017
SL Gr	Electrothermal effect	Si PhC	0.75/0.525	1.07	[135]	2017
SL Gr	Photothermal effect	Si <sub>3</sub> N <sub>4</sub> MRR	0.556/1.952	0.0079	[136]	2017
SL Gr	Electrothermal effect	Si PCNC	2.44/3.23	1.5	[62]	2017
BP film	Photothermal effect	Si MRR	0.479/0.113	0.0469	[78]	2020
b-AsP film	Electrothermal effect	Si MZI	30/20	0.74	[137]	2020
PtSe <sub>2</sub> film	photothermal effect	Si MRR	304/284	0.004	[140]	2020
SL Gr	photothermal effect	Si MRR	0.2/1.5	0.216	[141]	2021
SL Gr	photothermal effect	Si PCNC	3.24/5.52	0.0346	[142]	2021
SL Gr	photothermal effect	Si <sub>3</sub> N <sub>4</sub> MZI	1.25/2.83	0.0385	[143]	2021
SL Gr	Electrothermal effect	Si RTR	1.2/3.6	0.24	[144]	2022
MoTe <sub>2</sub> film	photothermal effect	Si MDR	1.5/3.3	0.1584	[138]	2023

<sup>a)</sup> Gr, Graphene; SL, single layer; BP, black phosphorus; b-AsP, black arsenic-phosphorus; <sup>b)</sup> MZI, Mach–Zehnder interferometer; MRR, microring resonator; MDR, microdisk resonator; ChG, chalcogenide glass; PhC, photonic crystal; PCNC, photonic crystal nanobeam cavity; RTR, racetrack-type resonator. <sup>c)</sup> The rise/full time follows the 10%–90% rule.

thermo-optic modulator with superior energy efficiency using a graphene heater has been demonstrated<sup>[79]</sup>. In addition, waveguide-integrated thermo-optic modulation based on a silicon photonic-crystal nanobeam cavity<sup>[62]</sup> with a 2D materials heater has also been demonstrated with reasonable results. All in all, both the experimental and simulation results have shown that graphene can work as an effective heat conductor for PICs, and the response time (rising time and decaying time) and the tuning efficiency (nm/mW or mW/FSR) of the thermal modulator are the most important parameters to consider when evaluating specific devices. A brief list of the performance of representative on-chip waveguide-integrated thermo-optic modulators is shown in Table 3.

Due to the intrinsically slow thermal diffusivity, the speed of thermo-optic modulation is limited to microseconds, whereas the modulation efficiency is usually much higher than the electro-optic effect, leading to devices with high extinction ratios, low ILs, and small footprints<sup>[17]</sup>. Meanwhile, thermo-optic modulation based on the photothermal effect greatly reduce thermal loads and heat leakage for the device. The response speed of these modulators based on the photothermal effect could be sub-microsecond, which provides a new approach to implementing high-efficiency thermo-optic tuning with a fast response. In fact, some 2D materials have optical absorption in the telecommunication band, resulting in degrading the modulation amplitude. Therefore, looking for 2D materials with broad bandgap and high thermal conductivity may also provide a possibility to realize a high-performance thermo-optic modulation. In conclusion, 2D-material-based thermo-optic modulators potentially offer a cost-effective solution for applications without the requirement of ultrafast modulation speed.

### 3.4. Hybrid 2D materials optical modulation with BICs

As discussed above, hybridizing 2D materials with PICs have many advantages, such as being free of lattice mismatch, low cost, and CMOS compatibility, because of the unique structure of 2D materials, which are formed by a single layer or several layers of atoms. However, there are still sev-

eral challenges in integrating 2D materials with high quality. The most straightforward method to integrate 2D materials is to transfer a 2D membrane onto prefabricated PICs<sup>[145, 146]</sup>, while the non-planarized topology of PICs will introduce strain and stress to 2D materials, which can cause 2D materials to crack at the edges of the waveguides. This will result in more phonon scattering centers, reduced electron mobility, and possible degradation of device performance. Although the non-planarized topology of PICs can be planarized by additional processing through the deposition of low-refractive-index dielectrics followed by chemical-mechanical polishing<sup>[60, 101, 147–149]</sup>, such processes are not only complex but will also reduce the optical overlap with the 2D materials. Another integration method is to grow thin-film dielectric materials on 2D materials and then fabricate micro/nano photonic structures with lithography methods<sup>[79, 150–152]</sup>. However, the properties of both the thin-film dielectrics and 2D materials are usually adversely affected<sup>[153–156]</sup>, such that single-crystal dielectric layers cannot be grown on 2D materials due to lattice mismatch and 2D materials will be damaged by high-energy plasma during deposition.

Recently, Yu *et al.* proposed an integration scheme utilizing BICs, as shown in Fig. 6(a)<sup>[103]</sup>. The BIC-based PICs enable light guided by a low-refractive-index waveguide on a high-refractive-index substrate with neglectable propagation losses<sup>[157, 158]</sup>, where the guided optical mode of TM polarization falls in the continuum spectrum of TE polarization (see the right-hand part of Fig. 6(a)). Thus, 2D materials can be transferred onto the flat single-crystal dielectric substrate before the fabrication of low-refractive-index polymer waveguides. The polymer manufacturing process does not involve high-energy plasma, allowing 2D materials to retain their initial properties after manufacturing. Utilizing the BIC-based integration scheme, Yu *et al.* recently demonstrated graphene thermo-optic modulation as shown in Fig. 6(b), where graphene was used as a heater<sup>[103]</sup>. Graphene electro-optic modulators were also demonstrated with the BIC-based integration scheme. Fig. 6(c) shows the structure of the fabri-

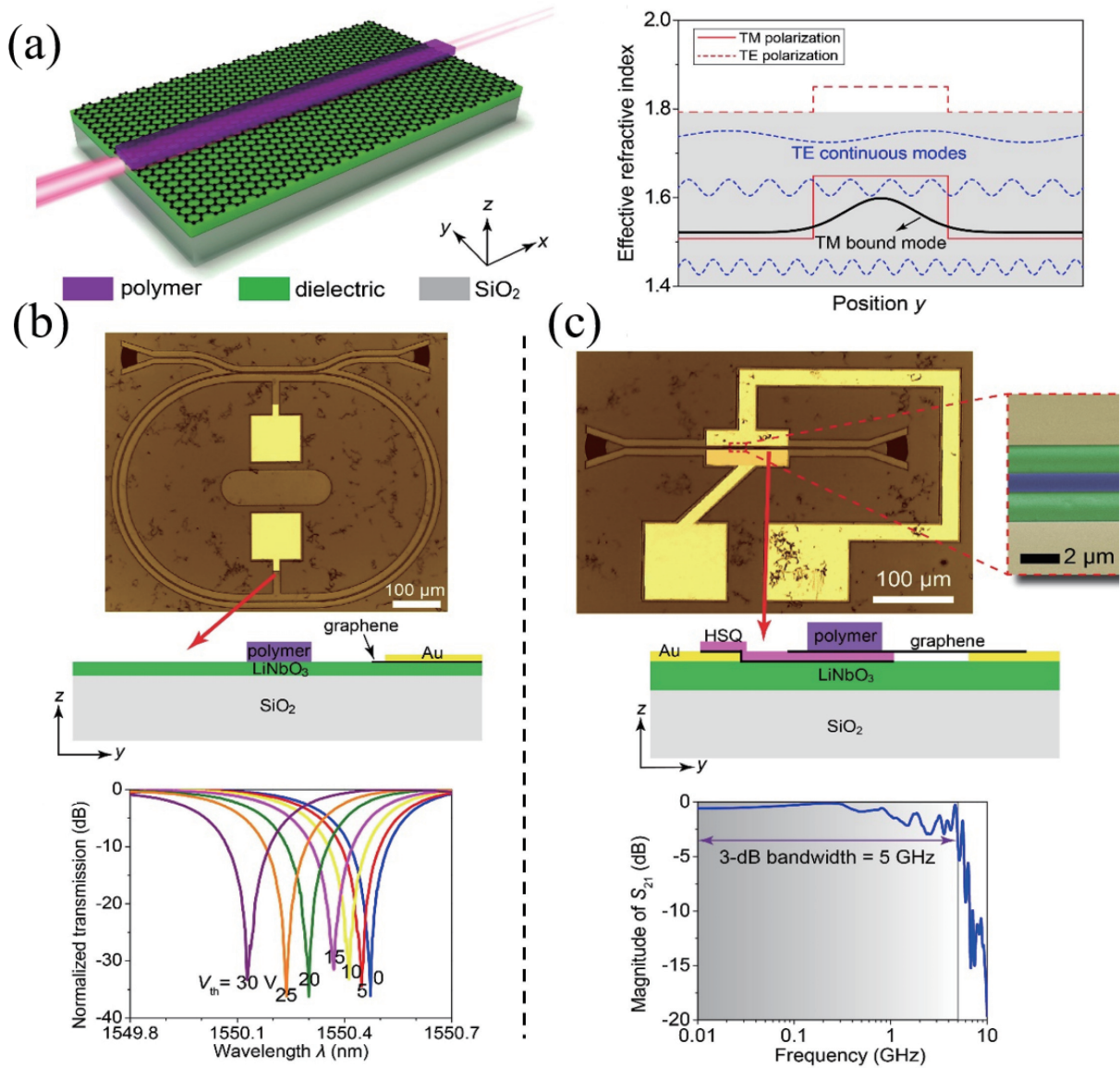


Fig. 6. (Color online) Hybrid 2D materials modulation with BICs. (a) Conceptual illustration of the integration scheme based on BICs (left-hand) and the effective-refractive-index wells for the TE/TM polarizations of light at  $1.55 \mu\text{m}$  in the hybrid waveguide (right-hand)<sup>[103]</sup>. (b) Optical microscope image and the cross-section of the fabricated thermo-optic modulator using graphene as heater based on the BICs scheme (upper part) and the measured transmission spectral response under different voltages (lower part)<sup>[103]</sup>. (c) Optical microscope image and the cross-section of the fabricated electro-optic modulator utilizing the electro-absorption effect of graphene based on the BICs scheme (upper part) and the measured frequency response ( $S_{21}$ ) of the device (lower part)<sup>[103]</sup>. Figures reproduced with permission: Ref. [103], © 2019 Wiley-VCH.

cated BIC-based waveguide-integrated electro-optic modulator<sup>[103]</sup>. The measured frequency response with a 3-dB bandwidth of  $\sim 5$  GHz is also shown. These findings imply that hybrid 2D materials PICs based on BICs open up a new avenue for 2D material integrated photonics and lay the groundwork for investigating new functional photonic devices on a chip, which will bring many previously unseen applications to PICs.

### 3.5. Hybrid 2D materials plasmonic waveguide optical modulation

Surface plasmon polaritons (SPPs) are well known for their ability to confine light far beyond the diffraction limit, which can significantly enhance the local light-matter interaction and is promising to play an important role in building up high-density PICs<sup>[159–163]</sup>. In addition, the relaxation time of SPPs is typically on the 10-fs level, which offers an

opportunity for realizing photonic devices with ultrafast responses<sup>[164]</sup>. The combination of 2D materials and plasmonic structures is promising to enable ultrafast, energy-efficient, and compact optical modulators. In addition, plasmonic structures can be efficiently integrated with silicon photonic waveguides through proper designs<sup>[165]</sup>, and thus hybrid waveguide-integrated optical modulation incorporating plasmonic structures and 2D materials has attracted a lot of attention recently.

Various hybrid plasmonic waveguide structures, including DL graphene<sup>[166, 167]</sup> and graphene nanoribbon<sup>[168]</sup>, have been theoretically studied, showing extraordinary properties. In 2017, Ding *et al.* experimentally demonstrated an electro-optic optical modulator based on a hybrid plasmonic waveguide loaded with graphene<sup>[58]</sup>, as schematically shown in Fig. 7(a), where the graphene sheet coupled with the leaky modes of the plasmonic slot waveguide and enhanced the

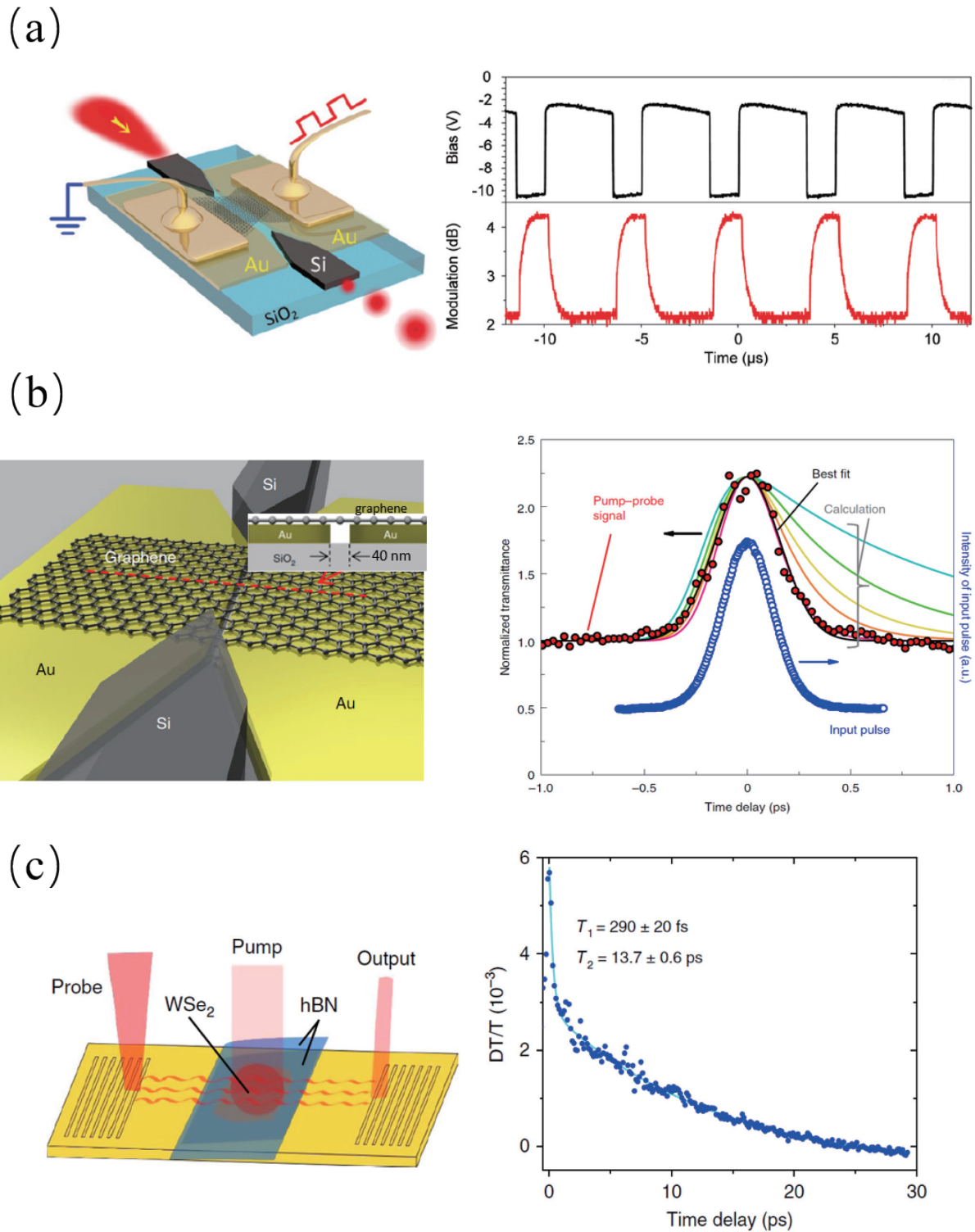


Fig. 7. (Color online) Hybrid plasmonic waveguide optical modulators with 2D materials. (a) Schematic illustration of an electro-optic modulator with a plasmonic waveguide loaded with graphene (left-hand) and the output optical signal under modulated bias (right-hand)<sup>[58]</sup>. (b) Schematic illustration of an all-optical modulator based on a plasmonic waveguide loaded with graphene (left-hand) and its pump-probe response (right-hand)<sup>[59]</sup>. (c) Schematic illustration of an all-optical plasmonic modulator based on 2D semiconductors (left-hand) and the transient time response of the device (right-hand)<sup>[121]</sup>. Figures reproduced with permission: (a) Ref. [58], © 2017 Royal Society of Chemistry. (b) Ref. [59], © 2020 Nature Publishing Group. (c) Ref. [121], © 2019 Nature Publishing Group.

light-matter interaction dramatically. This device achieved an MD of 0.13 dB/μm. The input electrical square waveform and the output optical signal for a 20-μm-long plasmonic slot waveguide are shown in the right-hand part of Fig. 7(a). Later, a hybrid plasmonic waveguide combined with graphene for electro-optic modulation with an ultra-com-

pact footprint<sup>[169]</sup> and broadband response<sup>[170]</sup> has been proposed. Recently, Ono *et al.* demonstrated an all-optical switch using a graphene-loaded deep-subwavelength (30 × 20 nm<sup>2</sup>) plasmonic waveguide<sup>[59]</sup>, as shown in Fig. 7(b), where both the pump and signal beams were coupled into the plasmonic slot waveguide from a silicon photonic waveguide



through an efficient mode converter. Due to the extreme light confinement brought by the plasmonic slot waveguide, the optical nonlinear absorption in graphene was greatly enhanced. This device achieved all-optical modulation with an ultralow switching energy of 35 fJ and an ultrafast time of 260 fs. The pump-probe signal of the device using femtosecond pulses is shown in the right-hand part of Fig. 7(b). The energy-time product argument has so far been the best for experimentally demonstrating all-optical modulation.

Furthermore, a plasmonic modulator (a device that controls the amplitude or phase of propagating plasmons) using 2D materials as nonlinear media has triggered widespread interest. By tuning the graphene sheet through gating, Ansell *et al.* demonstrated a hybrid graphene plasmonic waveguide modulator with a reasonably high MD over  $0.03 \text{ dB}/\mu\text{m}$  working at telecom wavelengths<sup>[171]</sup>. In 2019, Kelin *et al.* reported a plasmonic modulator combining monolayer  $\text{WSe}_2$  with a metallic waveguide<sup>[121]</sup>, as shown in Fig. 7(c). This device shows a 73% transmission change due to the strong interaction between the SPPs and the excitons in the  $\text{WSe}_2$ . The authors realized an all-optical 2D semiconductor nonlinear plasmonic modulator with an ultrafast response time of 290 fs using both optical and SPPs pumps<sup>[121]</sup>. The corresponding time-resolved response of the device pumped near the exciton resonance is shown in the right-hand part of Fig. 6(c). The combination of 2D materials with plasmonic modulators opens a door for the applications of 2D materials and paves the way toward ultrafast plasmonic amplifiers and transistors with low energy consumption.

As discussed earlier, the introduction of a plasmonic structure can dramatically enhance the light-matter interaction and thus improve the performances of waveguide-integrated optical modulators with 2D materials. It is expected that hybrid plasmonic waveguide structures with novel designs will help to build optical modulators with improved performance in the future.

#### 4. Conclusion and outlook

We have reviewed the recent progress of waveguide-integrated optical modulators with 2D materials utilizing different mechanisms, including the electro-optic, all-optical, and thermo-optic effects. Overall, in the past decade, great efforts have been made in almost all aspects, including theoretical design, material preparation, modulator configuration, and integration technologies, to improve the performance of waveguide-integrated optical modulators with 2D materials. As a result, significant progress has been made in several aspects and the outcomes have unambiguously suggested the great potential of using 2D materials for on-chip optical modulation. For example, the experimentally demonstrated electro-optic modulation speed has increased from around 1 GHz<sup>[16]</sup> to tens of GHz<sup>[52, 60, 104]</sup> in a few years. However, the optical modulators should be further improved to satisfy the demands of realistic applications, and significant efforts are still required for careful material selection, optimal structural designs, and improved fabrication processes. For waveguide-integrated electro-optic modulators with 2D materials, the modulation bandwidth is mainly limited by the parasitic response, and thus further improvement is desirable by optimizing the device configurations to fully take advantage of

2D materials. Novel device designs are also required to further reduce energy consumption. One of the most attractive features for all-optical modulation is its ultrafast modulation speed. However, these modulation utilizing nonlinear photonic effects usually require high energy consumption due to the high threshold and weak nonlinear photonic effects. Therefore, it is desired to further reduce energy consumption by introducing novel working mechanisms or structural designs. Basically speaking, when using thermo-optic modulation, the modulation speed is quite limited by slow thermal diffusion. Meanwhile, high modulation speed can be obtained by shrinking the structure size, optimizing the pumping method, or introducing new 2D materials with high thermal conductivity, which is possible given the richness of 2D materials. Shrunk optical modulators have been realized using the hybrid plasmonic waveguide with 2D materials, and they have shown some potential for future applications. Here, we discuss some possible directions that could be explored to further improve the performance of waveguide-integrated optical modulators with 2D materials.

**(1) 2D materials beyond graphene.** So far, most of the demonstrated optical modulators are based on graphene. However, more than 1000 kinds of 2D materials with fascinating properties have been predicted<sup>[172]</sup>. In addition, heterostructures formed by stacking different kinds of materials together have shown exotic properties that are not shared by any 2D materials alone because their band structures can be significantly adjusted by the strong interaction at the interface of two or more kinds of 2D materials. There is plenty of room to explore other 2D materials and their heterostructures with high mobility, low propagation loss, and significant tunability to realize high-performance optical modulators. For example, waveguide-integrated TMDs-based optical modulators have shown strong electro-refractive responses with low IL in the near-infrared wavelength range<sup>[77]</sup>.

**(2) Hybrid structures using novel optical waveguide structures.** As discussed, various waveguide structures have been implemented to construct 2D materials optical modulators with decent performance. Meanwhile, new waveguide structures are being developed with improved light-matter interaction by using modified fabrication techniques. For example, metamaterial-inspired silicon photonic structures<sup>[173, 174]</sup> have shown many extraordinary properties, which might offer more opportunities to realize high-performance waveguide-integrated optical modulators. Meanwhile, hybrid plasmonic waveguide structures show the potential to greatly improve the performance of optical modulators and novel plasmonic structures made up of novel metals<sup>[175]</sup> with loss and the introduction of gain materials<sup>[176]</sup> might be able to further improve the performances of waveguide-integrated optical modulators.

**(3) Optical modulator beyond the telecommunication band.** So far, most of the demonstrated optical modulators work in the telecommunication band. While, 2D materials have a broadband response ranging from the violet to the terahertz range<sup>[69]</sup>, and an optical modulator beyond the telecommunication band has attracted more attention for emerging applications<sup>[177, 178]</sup>. Thus, it is appealing to explore waveguide-integrated optical modulators with 2D materials working in the wavelength range beyond the telecommunica-

tion band.

**(4) Optimization of interplayed parameters for realistic applications.** The key FOMs of optical modulators are highly interplayed parameters. For realistic applications, a trade-off is usually required. More efforts are expected to be made to optimize the structural design of 2D materials-based optical modulators to reach their full potential for realistic applications.

## Acknowledgments

The authors acknowledge funding support from the National Major Research and Development Program (2019YFB2203603), the National Science Fund for Distinguished Young Scholars (61725503), the National Natural Science Foundation of China (NSFC) (62275273, 11804387, and 91950205), the China Postdoctoral Science Foundation (2020M681847), and the Zhejiang Provincial Natural Science Foundation (LZ18F050001).

## References

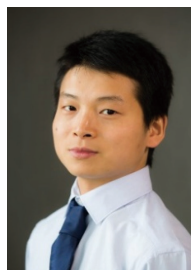
- [1] Srivastava N, Banerjee K. Interconnect challenges for nanoscale electronic circuits. *JOM*, 2004, 56, 30
- [2] Inniss D, Rubenstein R. Silicon photonics: fueling the next information revolution. Morgan Kaufmann, 2016
- [3] Wang J, Long Y. On-chip silicon photonic signaling and processing: A review. *Sci Bull*, 2018, 63, 1267
- [4] Thomson D, Zilkie A, Bowers J E, et al. Roadmap on silicon photonics. *J Opt*, 2016, 18, 073003
- [5] Guo D F, Hou K, Tang W J, et al. Silicon polarization switch based on symmetric polarization splitter-rotators. *J Semicond*, 2019, 40, 100401
- [6] Wang H M, Chai H Y, Lv Z R, et al. Silicon photonic transceivers for application in data centers. *J Semicond*, 2020, 41, 101301
- [7] Fu X, Dai D. Ultra-small Si-nanowire-based 400 GHz-spacing  $15 \times 15$  arrayed-waveguide grating router with microbends. *Electron Lett*, 2011, 47, 266
- [8] Bogaerts W, De Heyn P, Van Vaerenbergh T, et al. Silicon microring resonators. *Laser Photonics Rev*, 2012, 6, 47
- [9] Dai D X, Bauters J, Bowers J E. Passive technologies for future large-scale photonic integrated circuits on silicon: Polarization handling, light non-reciprocity and loss reduction. *Light Sci Appl*, 2012, 1, e1
- [10] Dai D X, Liu L, Gao S M, et al. Polarization management for silicon photonic integrated circuits. *Laser Photonics Rev*, 2013, 7, 303
- [11] Zhou Z P, Yin B, Michel J. On-chip light sources for silicon photonics. *Light Sci Appl*, 2015, 4, e358
- [12] Wang X, Su Z, Zhou Z. Recent progress of silicon photonics. *Scientia Sinica Physica*, 2015, 45, 014201
- [13] Bogaerts W, Chrostowski L. Silicon photonics circuit design: Methods, tools and challenges. *Laser Photonics Rev*, 2018, 12, 1700237
- [14] Liu S T, Khope A. Latest advances in high-performance light sources and optical amplifiers on silicon. *J Semicond*, 2021, 42, 041307
- [15] Reed G T, Mashanovich G, Gardes F Y, et al. Silicon optical modulators. *Nature Photon*, 2010, 4, 518
- [16] Liu M, Yin X B, Ulin-Avila E, et al. A graphene-based broadband optical modulator. *Nature*, 2011, 474, 64
- [17] Sun Z P, Martinez A, Wang F. Optical modulators with 2D layered materials. *Nature Photon*, 2016, 10, 227
- [18] Dai D X, Li J, Yin Y L. Silicon-plus photonics for light manipulation and photodetection. *Proc. SPIE 10812, Semiconductor Lasers and Applications VIII*, 2018, 1082
- [19] Wang X X, Liu J F. Emerging technologies in Si active photonics. *J Semicond*, 2018, 39, 061001
- [20] Su Y K, Zhang Y, Qiu C Y, et al. Silicon photonic platform for passive waveguide devices: Materials, fabrication, and applications. *Adv Mater Technol*, 2020, 5, 1901153
- [21] Marris-Morini D, Vakarín V, Ramirez J M, et al. Germanium-based integrated photonics from near- to mid-infrared applications. *Nanophotonics*, 2018, 7, 1781
- [22] Ramirez J M, Elfaiki H, Verole T, et al. III-V-on-silicon integration: From hybrid devices to heterogeneous photonic integrated circuits. *IEEE J Sel Top Quantum Electron*, 2020, 26, 1
- [23] Semond F. Epitaxial challenges of GaN on silicon. *MRS Bull*, 2015, 40, 412
- [24] Novoselov K S, Geim A K, Morozov S V, et al. Electric field effect in atomically thin carbon films. *Science*, 2004, 306, 666
- [25] Geim A K. Graphene: Status and prospects. *Science*, 2009, 324, 1530
- [26] Schaibley J R, Yu H Y, Clark G, et al. Valleytronics in 2D materials. *Nat Rev Mater*, 2016, 1, 16055
- [27] Manzeli S, Ovchinnikov D, Pasquier D, et al. 2D transition metal dichalcogenides. *Nat Rev Mater*, 2017, 2, 17033
- [28] Chen H, Liu M, Xu L, et al. Valley-selective directional emission from a transition-metal dichalcogenide monolayer mediated by a plasmonic nanoantenna. *Nanotechnol*, 2018, 9, 780
- [29] Jiang T, Yin K, Wang C, et al. Ultrafast fiber lasers mode-locked by two-dimensional materials: review and prospect. *Photonics Research*, 2020, 8(1), 78
- [30] Novoselov K S, Geim A K, Morozov S V, et al. Two-dimensional gas of massless Dirac fermions in graphene. *Nature*, 2005, 438, 197
- [31] Xia F N, Wang H, Xiao D, et al. Two-dimensional material nanophotonics. *Nat Photonics*, 2014, 8, 899
- [32] Caldwell J D, Aharonovich I, Cassaboís G, et al. Photonics with hexagonal boron nitride. *Nat Rev Mater*, 2019, 4, 552
- [33] Luo M M, Fan T J, Zhou Y, et al. 2D black phosphorus-based biomedical applications. *Adv Funct Mater*, 2019, 29, 1808306
- [34] Acun A, Zhang L, Bampoulis P, et al. Germanene: The germanium analogue of graphene. *J Phys: Condens Matter*, 2015, 27, 443002
- [35] Youngblood N, Li M. Integration of 2D materials on a silicon photonics platform for optoelectronics applications. *Nanophotonics*, 2016, 6, 1205
- [36] Akinwande D, Huyghebaert C, Wang C H, et al. Graphene and two-dimensional materials for silicon technology. *Nature*, 2019, 573, 507
- [37] Yin Y L, Li J, Xu Y, et al. Silicon-graphene photonic devices. *J Semicond*, 2018, 39, 061009
- [38] Dai D X, Li J, Song L J. Silicon-plus photonic devices for on-chip light-manipulation and photodetection. *Proc. SPIE 11182, Semiconductor Lasers and Applications IX*, 2019, 1118206
- [39] Tang Y H, Mak K F. 2D materials for silicon photonics. *Nature Nanotech*, 2017, 12, 1121
- [40] Chen H T, Nanz S, Abass A, et al. Enhanced directional emission from monolayer WSe<sub>2</sub> integrated onto a multiresonant silicon-based photonic structure. *ACS Photonics*, 2017, 4, 3031
- [41] Ross J S, Wu S F, Yu H Y, et al. Electrical control of neutral and charged excitons in a monolayer semiconductor. *Nat Commun*, 2013, 4, 1474
- [42] Ross J S, Klement P, Jones A M, et al. Electrically tunable excitonic light-emitting diodes based on monolayer WSe<sub>2</sub> p-n junctions. *Nat Nanotechnol*, 2014, 9, 268
- [43] Yang J, Xu R J, Pei J J, et al. Optical tuning of exciton and trion emissions in monolayer phosphorene. *Light Sci Appl*, 2015, 4, e312
- [44] Ouyang H, Chen H T, Tang Y X, et al. All-optical dynamic tuning of local excitonic emission of monolayer MoS<sub>2</sub> by integration

- with Ge<sub>2</sub>Sb<sub>2</sub>Te<sub>5</sub>. *Nanophotonics*, 2020, 9, 2351
- [45] Mouri S, Miyauchi Y, Matsuda K. Tunable photoluminescence of monolayer MoS<sub>2</sub> via chemical doping. *Nano Lett*, 2013, 13, 5944
- [46] Li Z W, Lv Y W, Ren L W, et al. Efficient strain modulation of 2D materials via polymer encapsulation. *Nat Commun*, 2020, 11, 1151
- [47] Novoselov K S, Mishchenko A, Carvalho A, et al. 2D materials and van der Waals heterostructures. *Science*, 2016, 353(6298), aac9439
- [48] Liu Y, Weiss N O, Duan X D, et al. Van der waals heterostructures and devices. *Nat Rev Mater*, 2016, 1, 16042
- [49] Gibertini M, Koperski M, Morpurgo A F, et al. Magnetic 2D materials and heterostructures. *Nat Nanotechnol*, 2019, 14, 408
- [50] Wei K, Jiang T, Xu Z J, et al. Hybrid perovskites: Ultrafast carrier transfer promoted by interlayer coulomb coupling in 2D/3D perovskite heterostructures (laser photonics rev. 12(10)/2018). *Laser Photonics Rev*, 2018, 12, 1870043
- [51] Wei K, Sui Y Z, Xu Z J, et al. Acoustic phonon recycling for photo-carrier generation in graphene-WS<sub>2</sub> heterostructures. *Nat Commun*, 2020, 11, 3876
- [52] Dalir H, Xia Y, Wang Y, et al. Athermal broadband graphene optical modulator with 35 GHz speed. *ACS Photonics*, 2016, 3, 1564
- [53] Mohsin M, Schall D, Otto M, et al. Graphene based low insertion loss electro-absorption modulator on SOI waveguide. *Opt Express*, 2014, 22, 15292
- [54] Lu Z L, Zhao W S. Nanoscale electro-optic modulators based on graphene-slot waveguides. *J Opt Soc Am B*, 2012, 29, 1490
- [55] Jiao J Y, Hao R, Zhen Z, et al. Optimization of graphene-based slot waveguides for efficient modulation. *IEEE J Sel Top Quantum Electron*, 2020, 26, 1
- [56] Cheng Z, Zhu X L, Galili M, et al. Double-layer graphene on photonic crystal waveguide electro-absorption modulator with 12 GHz bandwidth. *Nanophotonics*, 2020, 9, 2377
- [57] Shi Z, Gan L, Xiao T H, et al. All-optical modulation of a graphene-cladded silicon photonic crystal cavity. *ACS Photonics*, 2015, 2, 1513
- [58] Ding Y, Guan X, Zhu X, et al. Efficient electro-optic modulation in low-loss graphene-plasmonic slot waveguides. *Nanoscale*, 2017, 9, 15576
- [59] Ono M, Hata M, Tsunekawa M, et al. Ultrafast and energy-efficient all-optical switching with graphene-loaded deep-sub-wavelength plasmonic waveguides. *Nat Photonics*, 2020, 14, 37
- [60] Phare C T, Lee Y H D, Cardenas J, et al. Graphene electro-optic modulator with 30 GHz bandwidth. *Nat Photonics*, 2015, 9, 511
- [61] Gan S, Cheng C T, Zhan Y H, et al. A highly efficient thermo-optic microring modulator assisted by graphene. *Nanoscale*, 2015, 7, 20249
- [62] Xu Z Z, Qiu C Y, Yang Y X, et al. Ultra-compact tunable silicon nanobeam cavity with an energy-efficient graphene micro-heater. *Opt Express*, 2017, 25, 19479
- [63] Jafari Z, Zarifkar A, Miri M, et al. All-optical modulation in a graphene-covered slotted silicon nano-beam cavity. *J Light Technol*, 2018, 36, 4051
- [64] Chai Z, Hu X, Wang F, et al. Ultrafast All-Optical Switching. *Adv Opt Mater*, 2017, 5(7), 1600665
- [65] Yao Y H, Cheng Z, Dong J J, et al. Performance of integrated optical switches based on 2D materials and beyond. *Front Optoelectron*, 2020, 13, 129
- [66] Yu S L, Wu X Q, Wang Y P, et al. 2D materials for optical modulation: Challenges and opportunities. *Adv Mater*, 2017, 29, 1606128
- [67] Chen H T, Wang C, Ouyang H, et al. All-optical modulation with 2D layered materials: Status and prospects. *Nanophotonics*, 2020, 9, 2107
- [68] You J, Luo Y K, Yang J, et al. Hybrid/integrated silicon photonics based on 2D materials in optical communication nanosystems. *Laser Photonics Rev*, 2020, 14, 2000239
- [69] Gan X, Englund D, Van Thourhout D, et al. 2D materials-enabled optical modulators: From visible to terahertz spectral range. *Appl Phys Rev*, 2022, 9(2), 021302
- [70] Yang H Y, Wang Y Z, Tiu Z C, et al. All-optical modulation technology based on 2D layered materials. *Micromachines*, 2022, 13, 92
- [71] Wang G Z, Baker-Murray A A, Blau W J. Saturable absorption in 2D nanomaterials and related photonic devices. *Laser Photonics Rev*, 2019, 13, 1800282
- [72] Li Q, Lu J, Gupta P, et al. Engineering optical absorption in graphene and other 2D materials: Advances and applications. *Adv Opt Mater*, 2019, 7, 1900595
- [73] Cheng J L, Sipe J E, Vermeulen N, et al. Nonlinear optics of graphene and other 2D materials in layered structures. *J Phys Photonics*, 2018, 1, 015002
- [74] Wu K, Wang Y F, Qiu C Y, et al. Thermo-optic all-optical devices based on two-dimensional materials. *Photon Res*, 2018, 6, C22
- [75] Optical modulation. Cambridge University Press, Cambridge, 2016
- [76] Miller D A B. Energy consumption in optical modulators for interconnects. *Opt Express*, 2012, 20, A293
- [77] Datta I, Chae S H, Bhatt G R, et al. Low-loss composite photonic platform based on 2D semiconductor monolayers. *Nat Photonics*, 2020, 14, 256
- [78] Cheng Z, Cao R, Guo J, et al. Phosphorene-assisted silicon photonic modulator with fast response time. *Nanophotonics*, 2020, 9, 1973
- [79] Lin H T, Song Y, Huang Y Z, et al. Chalcogenide glass-on-graphene photonics. *Nature Photon*, 2017, 11, 798
- [80] Bao X Z, Ou Q D, Xu Z Q, et al. Band structure engineering in 2D materials for optoelectronic applications. *Adv Mater Technol*, 2018, 3, 1800072
- [81] Wang F, Zhang Y B, Tian C S, et al. Gate-variable optical transitions in graphene. *Science*, 2008, 320, 206
- [82] Liu Y P, Tom K, Wang X, et al. Dynamic control of optical response in layered metal chalcogenide nanoplates. *Nano Lett*, 2016, 16, 488
- [83] Liu M, Yin X B, Zhang X. Double-layer graphene optical modulator. *Nano Lett*, 2012, 12, 1482
- [84] Youngblood N, Anugrah Y, Ma R, et al. Multifunctional graphene optical modulator and photodetector integrated on silicon waveguides. *Nano Lett*, 2014, 14, 2741
- [85] Soriano V, Midrio M, Contestabile G, et al. Graphene-silicon phase modulators with gigahertz bandwidth. *Nat Photonics*, 2018, 12, 40
- [86] Agarwal H, Terrés B, Orsini L, et al. 2D-3D integration of hexagonal boron nitride and a high-κ dielectric for ultrafast graphene-based electro-absorption modulators. *Nat Commun*, 2021, 12, 1
- [87] Koester S J, Li M. High-speed waveguide-coupled graphene-on-graphene optical modulators. *Appl Phys Lett*, 2012, 100, 171107.
- [88] Hao R, Jin J M. Graphene embedded modulator with extremely small footprint and high modulation efficiency. *J Photonics*, 2014, 2014, 309350
- [89] Hao R, Ye Z W, Gu Y J, et al. Large modulation capacity in graphene-based slot modulators by enhanced hybrid plasmonic effects. *Sci Rep*, 2018, 8, 16830
- [90] Midrio M, Galli P, Romagnoli M, et al. Graphene-based optical phase modulation of waveguide transverse electric modes. *Photon Res*, 2014, 2, A34
- [91] Qiu C Y, Gao W L, Vajtai R, et al. Efficient modulation of 1.55 μm radiation with gated graphene on a silicon microring resonator. *Nano Lett*, 2014, 14, 6811
- [92] Ding Y H, Zhu X L, Xiao S S, et al. Effective electro-optical modulation with high extinction ratio by a graphene-silicon micror-



- ing resonator. *Nano Lett*, 2015, 15, 4393
- [93] Luo S Y, Wang Y N, Tong X, et al. Graphene-based optical modulators. *Nanoscale Res Lett*, 2015, 10, 1
- [94] Shi Y X, Li J S, Zhang L. Graphene-integrated split-ring resonator terahertz modulator. *Opt Quantum Electron*, 2017, 49, 350
- [95] Xu C, Jin Y C, Yang L Z, et al. Characteristics of electro-refractive modulating based on graphene-oxide-silicon waveguide. *Opt Express*, 2012, 20, 22398
- [96] Yang L Z, Hu T, Hao R, et al. Low-chirp high-extinction-ratio modulator based on graphene-silicon waveguide. *Opt Lett*, 2013, 38, 2512
- [97] Hao R, Du W, Chen H S, et al. Ultra-compact optical modulator by graphene induced electro-refraction effect. *Appl Phys Lett*, 2013, 103, 061161
- [98] Mohsin M, Neumaier D, Schall D, et al. Experimental verification of electro-refractive phase modulation in graphene. *Sci Rep*, 2015, 5, 10967
- [99] Ye S W, Wang Z S, Tang L F, et al. Electro-absorption optical modulator using dual-graphene-on-graphene configuration. *Opt Express*, 2014, 22, 26173
- [100] Gao Y D, Shiue R J, Gan X T, et al. High-speed electro-optic modulator integrated with graphene-boron nitride heterostructure and photonic crystal nanocavity. *Nano Lett*, 2015, 15, 2001
- [101] Hu Y T, Pantouvaki M, Van Campenhout J, et al. Broadband 10 Gb/s operation of graphene electro-absorption modulator on silicon. *Laser Photonics Rev*, 2016, 10, 307
- [102] Ye S W, Yuan F, Zou X H, et al. High-speed optical phase modulator based on graphene-silicon waveguide. *IEEE J Sel Top Quantum Electron*, 2017, 23, 76
- [103] Yu Z J, Wang Y, Sun B L, et al. Hybrid 2D-material photonics with bound states in the continuum. *Adv Optical Mater*, 2019, 7, 1901306
- [104] Luan C, Kong D M, Ding Y H, et al. High-modulation-efficiency graphene-silicon slot-waveguide micro-ring modulator. *Conference on Lasers and Electro-Optics, San Jose, 2022*
- [105] Gosciński J, Tan D T H. Theoretical investigation of graphene-based photonic modulators. *Sci Rep*, 2013, 3, 1897
- [106] Gan X T, Zhao C Y, Wang Y D, et al. Graphene-assisted all-fiber phase shifter and switching. *Optica*, 2015, 2, 468
- [107] Lee E J, Choi S Y, Jeong H, et al. Active control of all-fibre graphene devices with electrical gating. *Nat Commun*, 2015, 6, 6851
- [108] Hu Y Z, You J, Tong M Y, et al. Metaphotonic devices: Pump-color selective control of ultrafast all-optical switching dynamics in metaphotonic devices (adv. sci. 14/2020). *Adv Sci*, 2020, 7, 2070080
- [109] Bao Q L, Zhang H, Wang Y, et al. Atomic-layer graphene as a saturable absorber for ultrafast pulsed lasers. *Adv Funct Mater*, 2009, 19, 3077
- [110] Sun Z P, Hasan T, Torrisi F, et al. Graphene mode-locked ultrafast laser. *ACS Nano*, 2010, 4, 803
- [111] Zhang B T, Liu J, Wang C, et al. Recent progress in 2D material-based saturable absorbers for all solid-state pulsed bulk lasers. *Laser Photonics Rev*, 2020, 14, 1900240
- [112] Hendry E, Hale P J, Moger J, et al. Coherent nonlinear optical response of graphene. *Phys Rev Lett*, 2010, 105, 097401
- [113] Wang J, Hernandez Y, Lotya M, et al. Broadband nonlinear optical response of graphene dispersions. *Adv Mater*, 2009, 21, 2430
- [114] Bao Q L, Zhang H, Wang B, et al. Broadband graphene polarizer. *Nat Photonics*, 2011, 5, 411
- [115] Yu L H, Zheng J J, Xu Y, et al. Local and nonlocal optically induced transparency effects in graphene-silicon hybrid nanophotonic integrated circuits. *ACS Nano*, 2014, 8, 11386
- [116] Ooi K J A, Leong P C, Ang L K, et al. All-optical control on a graphene-on-silicon waveguide modulator. *Sci Rep*, 2017, 7, 1
- [117] Demongodin P, El Dirani H, Lhuillier J, et al. Ultrafast saturable absorption dynamics in hybrid graphene/Si<sub>3</sub>N<sub>4</sub> waveguides. *APL Photonics*, 2019, 4, 076102
- [118] Wang H, Yang N N, Chang L M, et al. CMOS-compatible all-optical modulator based on the saturable absorption of graphene. *Photon Res*, 2020, 8, 468
- [119] Chen H T, Corbaliou V, Solntsev A S, et al. Enhanced second-harmonic generation from two-dimensional MoSe<sub>2</sub> on a silicon waveguide. *Light Sci Appl*, 2017, 6, e17060
- [120] Yang S, Liu D C, Tan Z L, et al. CMOS-compatible WS<sub>2</sub>-based all-optical modulator. *ACS Photonics*, 2018, 5, 342
- [121] Klein M, Badada B H, Binder R, et al. 2D semiconductor nonlinear plasmonic modulators. *Nat Commun*, 2019, 10, 3264
- [122] Sun F Y, Xia L P, Nie C B, et al. An all-optical modulator based on a graphene-plasmonic slot waveguide at 1550 nm. *Appl Phys Express*, 2019, 12, 042009
- [123] Sun F Y, Xia L P, Nie C B, et al. The all-optical modulator in dielectric-loaded waveguide with graphene-silicon heterojunction structure. *Nanotechnology*, 2018, 29, 135201
- [124] Alaloul M, Khurgin J B. High-performance all-optical modulator based on graphene-HBN heterostructures. *IEEE J Sel Top Quantum Electron*, 2022, 28, 1
- [125] Yu S L, Meng C, Chen B G, et al. Graphene decorated microfiber for ultrafast optical modulation. *Opt Express*, 2015, 23, 10764
- [126] Li W, Chen B G, Meng C, et al. Ultrafast all-optical graphene modulator. *Nano Lett*, 2014, 14, 955
- [127] Sun D, Wu Z K, Divin C, et al. Ultrafast relaxation of excited Dirac fermions in epitaxial graphene using optical differential transmission spectroscopy. *Phys Rev Lett*, 2008, 101, 157402
- [128] Dong P, Qian W, Liang H, et al. Thermally tunable silicon racetrack resonators with ultralow tuning power. *Opt Express*, 2010, 18, 20298
- [129] Dong P, Shafiiha R, Liao S R, et al. Wavelength-tunable silicon microring modulator. *Opt Express*, 2010, 18, 10941
- [130] Renteria J, Nika D, Balandin A. Graphene thermal properties: Applications in thermal management and energy storage. *Appl Sci*, 2014, 4, 525
- [131] Kang J M, Kim H, Kim K S, et al. High-performance graphene-based transparent flexible heaters. *Nano Lett*, 2011, 11, 5154
- [132] Yu L H, Shi Y C, He S L, et al. Tunable silicon micro-disk resonator with flexible graphene-based ultra-thin heaters. *Asia Communications and Photonics Conference 2015, 2015, AS3B.2*
- [133] Yu L, He S, Zheng J, et al. Graphene-based transparent nanoheater for thermally-tuning silicon nanophotonic integrated devices. *Progress in Electromagnetics Research Symposium*, 2014, 1735
- [134] Yu L H, Yin Y L, Shi Y C, et al. Thermally tunable silicon photonic microdisk resonator with transparent graphene nanoheaters. *Optica*, 2016, 3, 159
- [135] Yan S Q, Zhu X L, Frandsen L H, et al. Slow-light-enhanced energy efficiency for graphene microheaters on silicon photonic crystal waveguides. *Nat Commun*, 2017, 8, 14411
- [136] Qiu C Y, Yang Y X, Li C, et al. All-optical control of light on a graphene-on-silicon nitride chip using thermo-optic effect. *Sci Rep*, 2017, 7, 17046
- [137] Liu Y J, Wang H D, Wang S, et al. Highly efficient silicon photonic microheater based on black arsenic-phosphorus. *Adv Optical Mater*, 2020, 8, 1901526
- [138] Cao H Y, Chen H T, Pan Y, et al. Efficient and fast all-optical modulator with *in situ* grown MoTe<sub>2</sub> nanosheets on silicon. *ACS Appl Nano Mater*, 2023, 6, 838
- [139] Yu L H, Dai D X, He S L. Graphene-based transparent flexible heat conductor for thermally tuning nanophotonic integrated devices. *Appl Phys Lett*, 2014, 105, 251104
- [140] Wei K K, Li D L, Lin Z T, et al. All-optical PtSe<sub>2</sub> silicon photonic modulator with ultra-high stability. *Photon Res*, 2020, 8, 1189
- [141] Li Z W, Liu Q, Wang H, et al. Photo-induced thermo-optical refraction switching by a graphene-assisted silicon microring resonator. *J Light Technol*, 2021, 39, 3471

- [142] Guo T, Gao S, Zeng H Y, et al. All-optical control of a single resonance in a graphene-on-silicon nanobeam cavity using thermo-optic effect. *J Light Technol*, 2021, 39, 4710
- [143] Qiu C Y, Zhang C, Zeng H Y, et al. High-performance graphene-on-silicon nitride all-optical switch based on a Mach-Zehnder interferometer. *J Light Technol*, 2021, 39, 2099
- [144] Nakamura S, Sekiya K, Matano S, et al. High-speed and on-chip optical switch based on a graphene microheater. *ACS Nano*, 2022, 16, 2690
- [145] Bonaccorso F, Sun Z, Hasan T, et al. Graphene photonics and optoelectronics. *Nat Photonics*, 2010, 4, 611
- [146] Gruhler N, Benz C, Jang H, et al. High-quality Si<sub>3</sub>N<sub>4</sub> circuits as a platform for graphene-based nanophotonic devices. *Opt Express*, 2013, 21, 31678
- [147] Gan X T, Shiue R J, Gao Y D, et al. Chip-integrated ultrafast graphene photodetector with high responsivity. *Nat Photonics*, 2013, 7, 883
- [148] Li H, Anugrah Y, Koester S J, et al. Optical absorption in graphene integrated on silicon waveguides. *Appl Phys Lett*, 2012, 101, 111110
- [149] Schall D, Neumaier D, Mohsin M, et al. 50 GBit/s photodetectors based on wafer-scale graphene for integrated silicon photonic communication systems. *ACS Photonics*, 2014, 1, 781
- [150] Nyakiti L O, Wheeler V D, Garces N Y, et al. Enabling graphene-based technologies: Toward wafer-scale production of epitaxial graphene. *MRS Bull*, 2012, 37, 1149
- [151] Huang C C, Al-Saab F, Wang Y D, et al. Scalable high-mobility MoS<sub>2</sub> thin films fabricated by an atmospheric pressure chemical vapor deposition process at ambient temperature. *Nanoscale*, 2014, 6, 12792
- [152] Zhou L, Xu K, Zubair A, et al. Large-area synthesis of high-quality uniform few-layer MoTe<sub>2</sub>. *J Am Chem Soc*, 2015, 137, 11892
- [153] Colombo L, Wallace R M, Ruoff R S. Graphene growth and device integration. *Proc IEEE*, 2013, 101, 1536
- [154] Lee B, Mordi G, Kim M J, et al. Characteristics of high-k Al<sub>2</sub>O<sub>3</sub> dielectric using ozone-based atomic layer deposition for dual-gated graphene devices. *Appl Phys Lett*, 2010, 97, 043107
- [155] Williams J R, DiCarlo L, Marcus C M. Quantum Hall effect in a gate-controlled *p-n* junction of graphene. *Science*, 2007, 317, 638
- [156] Wang X R, Tabakman S M, Dai H J. Atomic layer deposition of metal oxides on pristine and functionalized graphene. *J Am Chem Soc*, 2008, 130, 8152
- [157] Yu Z J, Xi X, Ma J W, et al. Photonic integrated circuits with bound states in the continuum. *Optica*, 2019, 6, 1342
- [158] Yu Z J, Tong Y Y, Tsang H K, et al. High-dimensional communication on etchless lithium niobate platform with photonic bound states in the continuum. *Nat Commun*, 2020, 11, 2602
- [159] Barnes W L, Dereux A, Ebbesen T W. Surface plasmon sub-wavelength optics. *Nature*, 2003, 424, 824
- [160] Bozhevolnyi S I, Volkov V S, Devaux E, et al. Channel plasmon subwavelength waveguide components including interferometers and ring resonators. *Nature*, 2006, 440, 508
- [161] Gramotnev D K, Bozhevolnyi S I. Plasmonics beyond the diffraction limit. *Nature Photon*, 2010, 4, 83
- [162] Chen H T, Yang J, Rusak E, et al. Manipulation of photoluminescence of two-dimensional MoSe<sub>2</sub> by gold nanoantennas. *Sci Rep*, 2016, 6, 22296
- [163] He W B, Chen H T, Ouyang H, et al. Tunable anisotropic plasmon response of monolayer GeSe nanoribbon arrays. *Nanoscale*, 2020, 12, 16762
- [164] MacDonald K F, Sámson Z L, Stockman M I, et al. Ultrafast active plasmonics. *Nat Photonics*, 2009, 3, 55
- [165] Ono M, Taniyama H, Xu H, et al. Deep-subwavelength plasmonic mode converter with large size reduction for Si-wire waveguide. *Optica*, 2016, 3, 999
- [166] Huang B H, Lu W B, Li X B, et al. Waveguide-coupled hybrid plasmonic modulator based on graphene. *Appl Opt*, 2016, 55, 5598
- [167] Gosciniaik J, Tan D T H. Graphene-based waveguide integrated dielectric-loaded plasmonic electro-absorption modulators. *Nanotechnology*, 2013, 24, 185202
- [168] Kim J T, Chung K H, Choi C G. Thermo-optic mode extinction modulator based on graphene plasmonic waveguide. *Opt Express*, 2013, 21, 15280
- [169] Rezaei M H, Zarifkar A. Graphene-based plasmonic electro-optical SR flip-flop with an ultra-compact footprint. *Opt Express*, 2020, 28, 25167
- [170] Shirdel M, Ali Mansouri-Birjandi M. A broadband graphene modulator based on plasmonic valley-slot waveguide. *Opt Quantum Electron*, 2020, 52, 36
- [171] Ansell D, Radko I P, Han Z, et al. Hybrid graphene plasmonic waveguide modulators. *Nat Commun*, 2015, 6, 8846
- [172] Mounet N, Gibertini M, Schwaller P, et al. Two-dimensional materials from high-throughput computational exfoliation of experimentally known compounds. *Nat Nanotechnol*, 2018, 13, 246
- [173] Staude I, Schilling J. Metamaterial-inspired silicon nanophotonics. *Nature Photon*, 2017, 11, 274
- [174] Xu H N, Dai D X, Shi Y C. Ultra-broadband and ultra-compact on-chip silicon polarization beam splitter by using hetero-anisotropic metamaterials. *Laser Photonics Rev*, 2019, 13, 1800349
- [175] Wang Y, Yu J Y, Mao Y F, et al. Stable, high-performance sodium-based plasmonic devices in the near infrared. *Nature*, 2020, 581, 401
- [176] Dai D X, Shi Y C, He S L, et al. Gain enhancement in a hybrid plasmonic nano-waveguide with a low-index or high-index gain medium. *Opt Express*, 2011, 19, 12925
- [177] Liang G Z, Huang H Q, Mohanty A, et al. Robust, efficient, micrometre-scale phase modulators at visible wavelengths. *Nat Photonics*, 2021, 15, 908
- [178] Pan B C, Hu J Y, Huang Y S, et al. Demonstration of high-speed thin-film lithium-niobate-on-insulator optical modulators at the 2- $\mu$ m wavelength. *Opt Express*, 2021, 29, 17710



**Haitao Chen** received his BS from the National University of Defense Technology (NUDT, China) in 2012 and PhD from Nonlinear Physics Center, the Australian National University (ANU, Australia) in 2018. He then joined the National University of Defense Technology as a lecturer. He worked at Daoxin Dai Group in Zhejiang University (ZJU, China) as a visiting postdoctoral fellow during the years 2020–2022. His research interests include silicon integrated nanophotonics, nonlinear photonics, and 2D materials photonics.



**Daoxin Dai** received his BS from Zhejiang University (ZJU, China) in 2000 and PhD from the Royal Institute of Technology (KTH, Sweden) in 2005. Later, he joined ZJU as an assistant professor in Aug. 2007 and a full professor in 2011. He worked at Bowers Group in the University of California at Santa Barbara (UCSB) as a visiting scholar during the years 2008–2011. Currently, he is the Qiushi Distinguished Professor and leading the silicon integrated nanophotonics group at Zhejiang University. He serves as the Dean of Optical Science & Engineering of Zhejiang University and the Director of MOE Joint International Research Laboratory of Photonics @ ZJU.